Journal of Proteomics 174 (2018) 71–84

Contents lists available at ScienceDirect

Journal of Proteomics

journal homepage: www.elsevier.com/locate/jprot

Transcriptomics-guided bottom-up and top-down venomics of neonate and adult specimens of the arboreal rear-fanged Brown Treesnake, *Boiga irregularis*, from Guam

Davinia Pla[a,1], Daniel Petras[b,1], Anthony J. Saviola[a,c,1,2], Cassandra M. Modahl[c,1], Libia Sanz[a], Alicia Pérez[a], Elena Juárez[a], Seth Frietze[c,2], Pieter C. Dorrestein[b], Stephen P. Mackessy[c,*], Juan J. Calvete[a,**]

[a] *Laboratorio de Venómica Estructural y Funcional, Consejo Superior de Investigaciones Científicas, Valencia, Spain*
[b] *University of California San Diego, Skaggs School of Pharmacy & Pharmaceutical Sciences, 9500 Gilman Dr, La Jolla, CA 92093, USA*
[c] *School of Biological Sciences, University of Northern Colorado, 501 20th Street, CB 92, Greeley, CO 80639, USA*

ARTICLE INFO

Keywords:
Top-down snake venom proteomics
Venom gland transcriptome
Rear-fanged snake venomics
Brown Treesnake
Boiga irregularis from Guam
Ontogenetic shift in venom composition
Three-finger toxins
Venom phenotypes

ABSTRACT

The Brown Treesnake (*Boiga irregularis*) is an arboreal, nocturnal, rear-fanged venomous snake native to northern and eastern regions of Australia, Papua New Guinea and the Solomon Islands. It was inadvertently introduced onto the island of Guam during the late 1940's to early 1950's, and it has caused massive declines and extirpations of the native bird, lizard, and mammal populations. In the current study, we report the characterization of the venom proteome of an adult and a neonate *B. irregularis* specimens from Guam by a combination of venom gland transcriptomic and venomic analyses. Venom gland transcriptomic analysis of an adult individual identified toxins belonging to 18 protein families, with three-finger toxin isoforms being the most abundantly expressed transcripts, comprising 94% of all venom protein transcript reads. Transcripts for PIII-metalloproteinases, C-type lectins, cysteine-rich secretory proteins, acetylcholinesterases, natriuretic peptides, ficolins, phospholipase A_2 (PLA_2) inhibitors, PLA_2s, vascular endothelial growth factors, Kunitz-type protease inhibitors, cystatins, phospholipase Bs, cobra venom factors, waprins, SVMP inhibitors, matrix metalloproteinases, and hyaluronidases were also identified, albeit, at very low abundances ranging from 0.05% to 1.7% of the transcriptome. The venom proteomes of neonate and adult *B. irregularis* were also both overwhelmingly (78 and 84%, respectively) dominated by monomeric and dimeric 3FTxs, followed by moderately abundant (21% (N) and 13% (A)) CRISPs, low abundance (1% (N), 3% (A)) PIII-SVMPs, and very low abundance (< 0.01%) PLA_2 and SVMP inhibitors. The differences in relative toxin abundances identified between neonate and adult snakes likely correlates to shifts in prey preference between the two age classes, from nearly-exclusively lizards to lizards, birds and small mammals. Immunoaffinity antivenomics with experimentally designed rabbit anti-Brown Treesnake (anti-BTS) venom IgGs against homologous venom from adult snakes demonstrated that CRISPs, PIII-SVMPs, and 60–70% of 3FTxs were effectively immunocaptured. Western blot analysis showed that all venom proteins were recognized by anti-BTS IgGs, and cross-reactivity with other rear-fanged snake venoms was also observed. Incubation of anti-BTS venom IgGs with crude *B. irregularis* venom resulted in a significant decrease in proteolytic (SVMP) activity against azocasein. These results provide the first comparative venomic and antivenomic analysis of neonate and adult *B. irregularis* from Guam, further highlighting evolutionary trends in venom composition among rear-fanged venomous snakes.

Significance paragraph: The Brown Treesnake (*Boiga irregularis*) has caused extensive ecological and economic damage to the island of Guam where it has become a classic example of the negative impacts of invasive species. In the current study, we report the first combined transcriptomic and proteomic analysis of *B. irregularis* venom of Guam origin. The transcriptome of an adult snake contained toxin sequences belonging to 18 protein families, with three-finger toxin (3FTx) isoforms being the most abundant and representing 94% of all venom protein transcript reads. Our bottom-up and top-down venomic analyses confirmed that 3FTxs are the major components of *B. irregularis* venom, and a comparative analysis of neonate and adult venoms demonstrate a clear ontogenetic

* Correspondence to: S.P. Mackessy, School of Biological Sciences, University of Northern Colorado, 501 20th Street, CB 92, Greeley, CO 80639, USA.
** Correspondence to: J.J. Calvete, Laboratorio de Venómica Estructural y Funcional, Instituto de Biomedicina de Valencia, C.S.I.C., Jaime Roig 11, 46010 Valencia, Spain.
E-mail addresses: stephen.mackessy@unco.edu (S.P. Mackessy), jcalvete@ibv.csic.es (J.J. Calvete).
[1] These authors have made equal contribution to the work, and should be considered "first authors".
[2] Current Address: Department of Medical Laboratory and Radiation Sciences, University of Vermont, 302 Rowell, 106 Carrigan Drive, Burlington, Vermont 05405, USA.

https://doi.org/10.1016/j.jprot.2017.12.020
Received 28 September 2017; Received in revised form 18 December 2017; Accepted 26 December 2017
Available online 29 December 2017

shift in toxin abundance, likely driven by dietary variation between the two age classes. Second-generation antivenomics and Western blot analysis using purified anti-Brown Treesnake rabbit serum IgGs (anti-BTS IgGs) showed strong immunoreactivity toward *B. irregularis* venom. Interestingly, our anti-BTS IgGs did not cross-react with 3FTxs found in several other rear-fanged snake venoms, or against 3FTxs in the venom of the elapid *Ophiophagus hannah*, indicating that epitopes in these 3FTx molecules are quite distinct.

1. Introduction

The genus *Boiga* comprises 33–34 recognized species of venomous, opisthoglyphous colubrid snakes commonly known as the Cat-eyed Snakes because of their vertical pupils (http://www.reptile-database.org). The Brown Treesnake, *Boiga irregularis* (Colubridae, Bechstein 1802) [1], is a nocturnal, oviparous snake native to coastal areas of Northern Australia and a large number of islands in northwestern Melanesia, from Sulawesi in eastern Indonesia through Papua New Guinea and the Solomon Islands. Although primarily arboreal, the Brown Treesnake occupies a wide variety of habitats at elevations from sea level to 1200 m [2]. In its native range, the Brown Treesnake is a generalist feeder, preying upon birds, lizards (such as geckos and skinks) and their eggs, bats, rats and other small rodents [2,3]. Natural predators include monitor lizards, cobras, owls, and several mammals [4,5]. Adult *B. irregularis* average 1.4–1.5 m in length, although individuals reaching lengths of 2.3 m (females) and 3.1 m (males) have been reported on Guam [2]. On Guam, *B. irregularis* represents an invasive species, accidentally introduced to this tiny (544 square-kilometers) Pacific island situated in the Philippine Sea, roughly between New Guinea and Japan (13.2 to 13.7° N and 144.6 to 145.0° E). Brown Treesnakes most likely were transported with US military equipment from the neighbouring Papua New Guinea island around the time of the island's liberation by American forces in 1944 [6–11]. Recent research has confirmed a longstanding hypothesis [4] that the invasive population of *B. irregularis* originated from Manus Island in the Admiralty Islands archipelago of Papua New Guinea and was likely established by fewer than 10 individuals [12]. Although feral pigs and cats occasionally prey on *B. irregularis*, they have had minimal effects on the snake population [13]. In the absence of natural predators to limit its population, coupled with sufficient prey availability, the Guam population of Brown Treesnakes reached peak densities of > 100 snakes per hectare in the mid-1980's [4,14].

Sixty years after the unintentional introduction of Brown Treesnakes, Guam's topographical and ecological diversity has resulted in heterogeneity in population characteristics of the invasive species throughout the island [15]. Currently, the Brown Treesnake population on Guam is declining with an equilibrium population size predicted to be roughly 30 to 50 snakes per hectare [4]. This population decline is attributed to depleted food resources [14], clear evidence that the Brown Treesnake population on Guam has exceeded carrying capacity. However, in spite of its currently decreasing numbers, the Brown Treesnake has significantly threatened Guam's native forest vertebrate species, and was responsible for devastating the indigenous populations of birds, lizards, and shrews during the mid-1980's [6–11,16,17]. Predation by introduced *B. irregularis* has resulted in the extinction of twelve native bird species and huge population declines of eight more [10,18]. Notably, the extinction of Guam's frugivore avifauna has led to the cessation of dispersal of native seeds, thereby affecting the mechanism of recolonization of degraded forests by native plants [14,19].

The pharmacology, toxinology, biochemistry, and toxin composition of venoms are, in general, much less studied in rear-fanged 'colubrids' than in front-fanged snakes [20,21]. However, over the past four decades, venoms from several *Boiga* species, including *B. blandingi*, *B. dendrophila*, and *B. irregularis*, have been shown to contain postsynaptic neurotoxic inhibitory activity [22–26]. Venom of *B. irregularis* possesses a prominent covalently linked heterodimeric 3FTx, irditoxin (PDB ID: 2H7Z), that exhibits potent and taxon-specific postsynaptic neurotoxicity. Irditoxin has been shown to be lethal to lizards and chicks, with LD_{50} values of 0.55 and 0.22 μg/g, respectively, but non-toxic to mice at doses up to 25 μg/g [25,26] (LD_{50} of whole venom toward inbred mice, 10–80 μg/g [27–29]). A recent combined venom proteomic and venom gland transcriptomic analysis [30] has confirmed the predominance of 3FTxs in the venom of a *B. irregularis* specimen from Indonesia. The weak neurotoxicity toward mammalian prey [26] likely underlies the lack of significant envenomation effects in adult humans [27,28], although symptoms requiring medical attention have been reported in extended contact bites to children [31]. The toxinological data correlate with the feeding ecology of *B. irregularis:* the snake uses its neurotoxic venom to subdue and kill avian and saurian prey, but constricts mammalian prey [25,32].

The larger *Boiga* species often exhibit an ontogenetic dietary shift from ectotherms to endotherms [3,7]. In the case of *B. irregularis*, the LD_{50} to lizard prey, particularly *Hemidactylus* geckos, increases from 1.1 μg/g in neonates to 2.5 μg/g in adults [25]. Previous biochemical analyses of *B. irregularis* venom indicated an ontogenetic shift from low to high enzymatic activity of snake venom metalloproteinases (SVMPs) and acetylcholinesterase (AchE) with increased snake size [25]. Further, low kallikrein-like, L-amino acid oxidase (LAAO), and phosphodiesterase (PDE) activity has also been documented [27]. The purpose of the work reported here was to perform venom gland transcriptomic (adult snake) and comparative proteomic analyses (neonate and adult) of the venoms of the Brown Treesnake from Guam in order to define at the molecular level the ontogenetic shift in venom composition.

2. Materials and methods

2.1. B. irregularis venoms

The venoms of one neonate (< 600 mm snout-vent length (SVL)) and one adult (> 1200 mm SVL) *B. irregularis* collected on Guam were manually extracted following methods developed by Hill and Mackessy [33]. Prior to venom extraction, snakes were anesthetized with ketamine–HCl (20 mg/kg), and then received an injection with pilocarpine (6 mg/kg) to stimulate venom flow. Venoms were collected *via* micropipettes, immediately centrifuged at 10,000 × *g* for 5 min to pellet insoluble material, frozen, lyophilized and stored at − 20 °C until used.

2.2. RNA isolation, library preparation and next-generation sequencing

Four days following venom extraction, a second adult *B. irregularis* originating from Guam was humanely euthanized and venom glands removed. All procedures were approved by the University of Northern Colorado Institutional Animal Care and Use Committee, IACUC protocol #9204.1. Approximately 50 mg of combined left and right venom gland tissue was homogenized in TRIzol (Life Technologies, USA), and RNA was isolated following the TRIzol manufacturer's protocol, with an additional overnight incubation in 300 μL 100% ethanol and 40 μL 3 M sodium acetate at − 20 °C to improve RNA yields. RNA yield was quantified using a Qubit 2.0 Fluorometer and RNA HS Assay kit (Thermo Fisher Scientific, USA). Total RNA (1 μg) was used as input into the NEBNext Ultra RNA library prep kit (New England BioLabs Inc., USA) for Oligo $d(T)_{25}$ bead poly-A tail selection. Fragmentation was performed to obtain approximately 200 bp insert sizes within the final library. First and second strand cDNA synthesis, adaptor ligation, and AMPure XP bead (Beckman Coulter, USA) clean-up steps were

completed following the NEBNext Ultra RNA library prep manufacturer's protocol for Illumina sequencing. The minimum number of recommended PCR cycles (12) was performed and the final AMPure XP bead purified library was assessed on a Bioanalyzer Agilent 2100 system (Agilent Technologies, USA) for proper fragment size selection and quality. This library was then equally pooled after qPCR KAPA library quantification (KAPA Biosystems, USA) with four other uniquely barcoded libraries and sequenced on a single HiSeq 2500 instrument lane at the Genomics and Microarray Core Facility (University of Colorado Anschutz Medical Campus) to obtain 125 bp paired-end reads.

2.3. Transcriptome assembly, annotation and toxin transcript quantification

Illumina reads were assessed using the Java program FastQC (Babraham Institute Bioinformatics, U.K.), and low quality reads (Phred + 33 score < 30) and contaminating adaptor sequences were removed using Trimmomatic with a sliding window of 4 bps [34]. To obtain a comprehensive venom gland transcriptome assembly, contigs from three different assemblies were used. First, a Trinity (release v2014-07-17) *de novo* assembly of paired-end reads was completed with default parameters (k-mer size 25) [35]. A second *de novo* assembly was completed with the program Extender (k-mer size 100) [36]. For the Extender assembly, reads were first merged with PEAR (Paired-End read mergeR v0.9.6 [37]; default parameters) if their 3′ ends overlapped to create longer contiguous sequences, and these merged reads were used as Extender input. The Extender assembly was performed with the same parameters as specified for the venom gland assembly of *B. irregularis* originating from Indonesia [30]. Lastly, a genome-guided Trinity (release v2014-07-17) assembly was performed using the available Indonesian *B. irregularis* venom gland assembly as a reference with Bowtie2 [38] used for generating the bam file input. These three approaches were taken to assemble contigs both shared and unique between snakes from Guam and Indonesia, as well as accounting for transcripts that are best assembled using short or long k-mers.

Contigs from these three assemblies were combined and BLASTx (executed using BLAST + command line (version 2.6.0); minimum *E*-value of 10^{-4}) [39] completed against a custom snake protein database, which consisted of all identified squamate venom proteins available in the NCBI databases (https://www.ncbi.nlm.nih.gov) (release 214, June 15, 2016, comprising over 73,700 entries, including all predicted protein sequences from the venom gland transcriptome of the Indonesia *B. irregularis*) venom gland transcriptome toxin and non-toxin protein sequences, and all predicted proteins from the genomes of *Ophiophagus hannah* and *Python bivittatus* [40,41]. In addition, BLASTx and BLASTn (version 2.6.0) [42] were performed against the NCBI nr and nt databases (downloaded March 2017), respectively, with the same *E*-value threshold for the identification of any novel transcripts not present in the custom database. To identify complete coding sequences (CDS), the resulting custom BLASTx output and all contigs were used as input files for standalone ORFpredictor [43]. Predicted CDS and protein sequences from contigs were clustered with CD-HIT to remove redundancy from using multiple assemblers [44,45]. Reads were mapped with Bowtie2 and transcript abundances determined using RSEM (RNA-seq by Expectation-Maximization; v1.2.23) [46]. Transcripts below a FPKM (Fragments Per Kilobase of transcript per Million mapped reads) value of 1 were excluded from the analysis, and TPM (Transcripts Per Million) values were used to report transcript abundances. Transcripts were reported as venom components if the resulting protein had a significant (*E*-value of 10^{-4}) BLASTx hit to a current venom protein, contained a signal peptide sequence and produced a translated full-length protein (partial protein transcripts were identified, but not reported).

To allow for a direct venom protein superfamily gene expression comparison between the two *B. irregularis* localities, transcripts identified as resulting in full-length venom proteins, GDBA00000000.1 contigs for Indonesian *B. irregularis* and the 110 contigs identified within this study for the Guam *B. irregularis* individual, were used as a reference for Bowtie2 read mapping (Sequence Read Archive accession codes SRR1292619 (Indonesian) and SRR6012492 (Guam) *B. irregularis*), and RSEM was used for transcript abundance quantification.

2.4. Isolation and initial characterization of venom proteins

Two mg (adult) and 1.5 mg (neonate) of crude lyophilized venom were dissolved in 300 μL of 0.05% trifluoroacetic acid (TFA) and 5% acetonitrile (ACN). Insoluble material was removed by centrifugation in an Eppendorff centrifuge at 13,000*g* for 10 min at room temperature, and the proteins contained in 15–20 μL were separated by RP-HPLC using a Teknokroma Europa C_{18} (250 × 4 mm, 5 μm particle size, 300 Å pore size) column and Agilent LC 1100 High Pressure Gradient System equipped with DAD detector. The flow-rate was set to 1 mL/min and the column was developed with a linear gradient of 0.1% TFA in water (solution A) and 0.1% TFA in ACN (solution B) and elution was achieved as follows: isocratically (5% B) for 5 min, followed by 5–25% B for 10 min, 25–45% B for 60 min, and 45–70% for 10 min. Protein detection was carried out at 215 nm with a reference wavelength of 400 nm. Fractions were collected manually across the entire elution range, dried in a vacuum centrifuge (Savant), and redissolved in water. Molecular masses of the purified proteins were estimated by non-reduced and reduced SDS-PAGE (on 12 or 15% polyacrylamide gels), or determined by electrospray ionization (ESI) mass spectrometry. For SDS-PAGE analysis sample aliquots were mixed with ¼ volume of 4 × sample buffer (0.25 M Tris-HCl pH 6.8, 8% SDS, 30% glycerol, 0.02% bromophenol blue, with or without 10% 2-mercaptoethanol) and heated at 85 °C for 15 min. For ESI-MS, sample aliquots were mixed 1:1 (v/v) with 70% acetonitrile containing 1% formic acid and analyzed in an Applied Biosystems QTrap™ 2000 mass spectrometer operated in Enhanced Multiple Charge mode in the range *m/z* 350–1700. Data were acquired and processed using Analyst 1.5.1. software (Framingham, MA, USA). All chromatographic fractions were submitted to SDS-PAGE analysis run under non-reducing and reducing conditions and the gels were stained with Coomassie Brilliant Blue G-250.

2.5. Bottom-up mass spectrometric characterization and quantification of the venom proteome of neonate and adult B. irregularis (Guam)

Chromatographic fractions containing peptides ($m/z \leq 1700$) were loaded in a nanospray capillary column and submitted to peptide sequencing using a QTrap™ 2000 mass spectrometer (Applied Biosystems) equipped with a nanospray source (Protana, Denmark). Mono, doubly- or triply-charged ions selected after enhanced resolution MS analysis were fragmented using the enhanced production with Q0 trapping option. Enhanced resolution was performed at 250 amu/s across the entire mass range. Q1 was operated at unit resolution, the Q1 to Q2 collision energy was set to 35–45 eV, the Q3 entry barrier was 8 V, the linear ion trap Q3 fill time was 250 ms, and the scan rate in Q3 was 1000 amu/s.

Data were acquired and processed using Analyst 1.5.1. software (Framingham, MA, USA). Production spectra were interpreted manually or using the on-line form of the MASCOT Server (version 2.6) at http://www.matrixscience.com against a private database containing all the snake venom protein sequences deposited in the non-redundant UniProt and NCBI (release 218, February 15, 2017) databases plus the protein sequences translated from the species-specific venom gland transcriptome. MS/MS mass tolerance was set to ± 0.6 Da. Oxidation of methionine was specified as variable modification. Spectra producing positive hits were manually inspected. Good quality spectra that did not match any known protein sequence were interpreted manually to derive *de novo* amino acid sequences. Amino acid sequence similarity

searches were performed at https://blast.ncbi.nlm.nih.gov/Blast.cgi against the non-redundant protein sequences database, using the default parameters of the BLASTP program [42].

Protein bands of interest were excised from Coomassie Brilliant Blue-stained SDS-PAGE gels and subjected to in-gel reduction (10 mM dithiothreitol, 30 min at 65 °C) and alkylation (50 mM iodacetamide, 2 h in the dark at room temperature), followed by overnight sequencing-grade trypsin digestion (66 ng/μL in 25 mM ammonium bicarbonate, 10% ACN; 0.25 μg/sample) in an automated processor (using a Genomics Solution ProGest Protein Digestion Workstation) following the manufacturer's instructions. Tryptic digests were dried in a vacuum centrifuge (SPD SpeedVac®, ThermoSavant), redissolved in 15 μL of 5% ACN containing 0.1% formic acid, and submitted to LC-MS/MS. To this end, tryptic peptides were separated by nano-Acquity UltraPerformance LC® (UPLC®) using BEH130 C18 (100 μm × 100 mm, 1.7 μm particle size) column in-line with a Waters SYNAPT G2 High Definition Mass Spectrometry System. The flow rate was set to 0.6 μL/min and column was develop with a linear gradient of 0.1% formic acid in water (solution A) and 0.1% formic acid in ACN (solution B), isocratically 1% B for 1 min, followed by 1–12% B for 1 min, 12–40% B for 15 min, 40–85% B for 2 min. Doubly and triply charged ions were selected for CID-MS/MS. Fragmentation spectra were interpreted i) manually (*de novo* sequencing), ii) using the on-line form of the MASCOT Server (version 2.6) at http://www.matrixscience.com against the last update (release 214, June 15, 2016) of NCBI non-redundant database, and iii) processed in Waters Corporation's ProteinLynx Global SERVER 2013 version 2.5.2. (with Expression version 2.0). The following search parameters were used: Taxonomy: all entries; enzyme: trypsin (1 missed cleavage allowed); MS/MS mass tolerance was set to ± 0.6 Da; carbamidomethyl cysteine and oxidation of methionine were selected as fixed and variable modifications, respectively. All matched MS/MS data were manually checked. Peptide sequences assigned by *de novo* MS/MS were matched to *B. irregularis* (Guam and Indonesia) transcriptomic datasets and/or to proteins available in the NCBI non-redundant protein sequences database using the default parameters of the BLASTP program [42].

The relative abundances of the chromatographic peaks obtained by reverse-phase HPLC fractionation of the whole venom were calculated by dividing the peak area by the total area of the chromatogram [47–49]. Recording at the absorbance wavelength for a peptide bond [190–230 nm], and applying the Lambert-Beer law (A = εcl, where A = absorbance; ε is the molar absorption [extinction] coefficient, [M^{-1} cm^{-1}]; c = concentration [M]; and l = length [cm] of the solution that light passes through), these percentages correspond to the "% of total peptide bond concentration in the peak". For chromatographic peaks containing single components (as judged by SDS-PAGE and/or MS), this figure is a good estimate of the % by weight (g/100 g) of the pure venom component. When more than one venom protein was present in a reverse-phase fraction, their proportions (% of total protein bands area) were estimated by densitometry of Coomassie-stained SDS-polyacrylamide gels using MetaMorph® Image Analysis Software (Molecular Devices). Conversely, the relative abundances of different proteins contained in the same SDS-PAGE band were estimated based on the relative ion intensities of the three most abundant peptide ions associated with each protein by MS/MS analysis. The relative abundances of the protein families present in the venom were calculated as the ratio of the sum of the percentages of the individual proteins from the same family to the total area of venom protein peaks in the reverse-phase chromatogram.

2.6. Top-down LC-MS/MS

For top-down mass spectrometry, the venoms of adult and neonates were dissolved in ultrapure water to a final concentration of 10 mg/mL, and centrifuged at 12,000*g* for 5 min. To reduce the disulfide bonds, 10 μL of venom was mixed with 10 μL of 0.5 M tris(2-carboxyethyl) phosphine (TCEP), and 30 μL of 0.1 M citrate buffer, pH 3, was added. After a 30 min incubation at 65 °C, samples were mixed with 50 μL of ACN/FA/H_2O 10:1:89 (v/v/v) and centrifuged at 12,000*g* for 5 min. After centrifugation, 5 μL of supernatant of reduced samples were submitted in duplicates to LC-MS/MS analyses. LC-MS/MS experiments of two technical replicates were performed on a Vanquish ultra-high performance liquid chromatography (UHPLC) system coupled to a Q-Exactive hybrid quadrupole orbital ion trap (Thermo Fisher Scientific, Bremen, Germany).

LC separation was performed on a Supelco Discovery Biowide C18 column (300 Å pore size, 2 × 150 mm column size, 3 μm particle size). A flow rate of 0.5 mL/min was used and the samples were eluted with a gradient of 0.1% formic acid (FA) in water (solution A) and 0.1% FA in ACN (solution B), isocratically with 5% B for 0.5 min, followed by an increase to 40% B for 50 min, and 40–70% B for 60 min. The column was washed with 70% B for 5 min and re-equilibrated at 5% B for 5 min. ESI settings were adjusted to 53 L/min sheath gas, 18 L/min auxiliary gas, spray voltage 3.5 kV, capillary voltage 63 V, S lens RF level 90 V, and capillary temperature 350 °C.

MS/MS spectra were obtained in data-dependent acquisition (DDA) mode. FTMS measurements were performed with 1 μ scan and 1000 ms maximal fill time. AGC targets were set to 10^6 for full scans and to 3×10^5 for MS/MS scans. The survey scan and data dependent MS/MS scans were performed with a mass resolution (R) of 140,000 (at *m/z* 200). For MS/MS, the three most abundant ions of the survey scan with known charge were selected for high energy C-trap dissociation (HCD) at the apex of a peak within 2 to 15 s from their first occurrence. Normalized collision energy was stepwise increased from 25% to 30% to 35%. The default charge state was set to z = 6, and the activation time to 30 ms. The mass window for precursor ion selection was set to 3 *m/z*. A window of 3 *m/z* was set for dynamic exclusion within 30 s. Ion species with unassigned charge states as well as isotope peaks were excluded from MS/MS experiments.

For data analysis, raw data were converted to .mzXML files using MSconvert of the ProteoWizard package (version 3.065.85) and multiple charged spectra were deconvoluted using MS-Deconv (version 0.8.0.7370). The maximum charge was set to 30, maximum mass was set to 50,000, signal-to-noise threshold was set to 2, and *m/z* tolerance was set to 0.02 amu. Protein spectra matching was performed using TopPIC (http://proteomics.informatics.iupui.edu/software/toppic/) [50] (version 1.0.0) against a non-redundant database comprising all NCBI *Boiga irregularis* sequences (3146) downloaded on 7 March 2017. Additionally, protein sequences of known typical contaminants from the common Repository of Adventitious Proteins (cRAP) were added to the database. TopPIC mass error tolerance was set to 10 ppm. A false discovery rate (FDR) cut-off was set to 0.01. Maximal allowed unexpected PTMs was set to one.

For the generation of intact mass extracted ion chromatograms (XICs) and manual validation of protein spectra matches, the MS raw data were deconvoluted using XTRACT of the Xcalibur Qual Browser version 2.2 (Thermo, Bremen, Germany). Intact mass feature findings of both mono-isotopic deconvoluted reduced and native LC-MS runs were performed with MZmine 2 (version 2.2). A 1.0e4 signal intensity threshold was used for peak selection. The mass alignment for the creation of XICs was performed with a minimum peak width of 30 s, and 3.0e4 peak height. Mass error tolerance was set to 10 ppm. For chromatographic deconvolution, the baseline cutoff algorithm with 1.0e4 signal threshold was used. Maximum peak width was set to 10 min. Feature alignment was performed with 10 ppm mass accuracy and 0.5 min retention time tolerance. The alignment of MS/MS protein ID from TopPic to MS1 XICs was performed with an in-house R script available as a jupyter notebook at https://github.com/DorresteinLaboratory/match_tables_by_exact_mass. For relative quantification, ion intensities were calculated using the area under the curve of XIC and used for downstream data analysis. Peak areas were normalized to TIC. *P*-values for fold change of XIC areas between adult and

neonates were calculated using *t*-test and their negative logarithm of 10 was plotted against the logarithm of 2 of the fold change.

2.7. Cladogram of 3FTxs identified in Guam and Indonesian venoms

Multiple sequence alignment of 3FTx sequences identified in Guam (this work) and Indonesiam [30] *B. irregularis* venom proteomes was completed using MEGA version 6.0.6 [51]. A neighbor-joining cladogram was constructed using the same software and default parameters.

2.8. Anti-Brown Treesnake (BTS) venom antibodies and antivenomics

An experimental antiserum was raised in rabbits by subcutaneous injections of adult Guam *B. irregularis* venom. The first injection comprised 250 μg venom in 250 μL of isotonic (0.9%) saline solution emulsified with an equal volume of Freund's complete adjuvant. Booster injections of the same amount of immunogen emulsified in Freund's incomplete adjuvant were administered at 3 week intervals for a period of 2 months. Terminal cardiac blood collection, performed by intracardiac puncture under general anesthesia, was approved by the IBV's Ethics Commission (074/2014-2019) and by the Generalitat Valenciana (2014/VSC/PEA/00060 tipo 2). Collected whole blood was allowed to clot by leaving it undisturbed at room temperature (RT) for 3 h. The clot was removed from serum by centrifugation for 45 min at 2000 × *g* using a refrigerated centrifuge. The serum pH was adjusted to 5.8 with 120 mM sodium acetate buffer (pH 4.0), and the IgG fraction was purified by slowly adding, under vigorous stirring of the serum, caprylic acid to a final concentration of 6% (v/v). The mixture was vigorously stirred for 90 min at RT followed by centrifugation at 5000 × *g* for 10 min [52]. The supernatant was extensively dialyzed (using Spectra/Por® Dialysis Tubing MWCO 20,000) against MilliQ® water and lyophilized.

A second-generation antivenomics approach [53] was applied to examine the paraspecific immunoreactivity of the rabbit anti-BTS IgGs against homologous venom from both adult and neonate snakes. To prepare the antivenom affinity column, 3 mL of CNBr-activated SepharoseTM 4B matrix (GE Healthcare) was packed in a Pierce centrifuge column and washed with 10 matrix volumes of cold 1 mM HCl followed by two matrix volumes of 0.2 M $NaHCO_3$, containing 0.5 M NaCl, pH 8.3 (coupling buffer) to adjust the pH of the column to 7.0–8.0. Seventy mg of lyophilized IgG was reconstituted in 4 mL of coupling buffer and the concentration of this stock solution was determined spectrophotometrically using a 1 cm light pathlength cuvette and an extinction coefficient of 1.36 at 280 nm for a 1 mg/mL protein concentration. Sixty mg of IgG was incubated with the CNBr-activated matrix for 4 h at RT. The coupling yield, which was estimated by measuring A_{280} before and after coupling of the antivenom was 48 mg (16 mg IgG/mL matrix). After the coupling, any remaining active groups were blocked with 300 μL of 0.1 M Tris-HCl, pH 8.5 at RT for 4 h. The column was alternately washed with 3 column volumes of 0.1 M acetate containing 0.5 M NaCl, pH 4.0–5.0, and 3 column volumes of 0.1 M Tris-HCl, pH 8.5 repeated 6 times. The column was then equilibrated with 5 volumes of working buffer solution (20 mM phosphate buffer, 135 mM NaCl, pH 7.4; PBS). For the immunoaffinity assay, increasing amounts (50 μg, 75 μg, 100 μg and 150 μg) of *B. irregularis* venom were dissolved in half matrix volumes of PBS and incubated with 300 μL of affinity matrix for 1 h at RT using an orbital shaker. As a specificity control, 300 μL of mock CNBr-activated SepharoseTM 4B matrix was incubated with 100 μg of venom and this control column was developed in parallel to the immunoaffinity experiment. Non-retained fractions were collected with 5 matrix volumes of PBS, and the immunocaptured proteins were eluted with 5 matrix volumes of elution buffer (0.1 M glycine-HCl, pH 2.0) and neutralised with 150 μL 1 M Tris-HCl, pH 9.0. The non-retained and the immunocaptured venom fractions were lyophilized, reconstituted in 40 μL of MilliQ® water, and fractionated by reverse-phase HPLC on a Discovery® BIO Wide Pore C_{18} (15 cm × 2.1 mm, 3 μm particle size, 300 Å pore size) column using an Agilent LC 1100 High Pressure Gradient System equipped with a DAD. The column was developed at a flow rate of 0.4 mL/min and proteins eluted with a linear gradient of 0.1% TFA in MilliQ® water (solution A) and 0.1% TFA in ACN (solution B): isocratic at 5% solution B for 1 min, followed by 5–25% solution B for 5 min, 25–45% solution B for 35 min, and 45–70% solution B for 5 min. Protein was detected at 215 nm with a reference wavelength of 400 nm. Proteins eluting in the non-retained and retained chromatographic fractions were identified by comparing the their masses determined by ESI-MS with the database generated by top-down LC-MS/MS.

2.9. Western blot analysis

Samples of venoms (8 μg/lane) from specimens of viperid (*Crotalus tzabcan*, Middle American rattlesnake; Yucatán Peninsula, México), elapid (*Ophiophagus hannah*, King cobra; Thailand) and rear-fanged snakes [*Ahaetulla prasina* (Asian vine snake; Indonesia: Sumatra); *Alsophis portoricensis* (Puerto Rican racer; Guana Island, British Virgin Islands); *Boiga cynodon* (Dog-toothed catsnake; Indonesia); *Boiga dendrophila* (mangrove snake; Indonesia); *Boiga irregularis* (Brown Treesnake, Guam); *Dispholidus typus* (South African Boomslang); *Hypsiglena jani* (Texas night snake; USA: southeastern Arizona); *Leioheterodon madagascariensis* (Madagascan giant hognose); *Oxybelis fulgidus* (Green vine snake; South America: Suriname); *Philodryas patagonensis* (Patagonia green racer: Argentina); *Thamnodynastes strigatus* (Coastal house snake; Brazil); *Thelornis kirtlandii* (Forest vine snake; Uganda); *Trimorphodon biscutatus lambda* (Sonoran lyre snake; Portal, AZ)], extracted as described previously [33,54], were subjected to Western blot analysis following reducing SDS-PAGE on 12% acrylamide NuPAGE® Bis-Tris precast gels [55]. Proteins were blotted to nitrocellulose (150 mA for 1.5 h), and the membrane was rinsed in Millipore-filtered water (18.2 MΩ cm MilliQ™ H_2O) and then blocked in PBS-buffered 3% BSA (Sigma Fraction V) for 1 h at RT. Membranes were rinsed 3 × in PBS and then incubated with 15 mL primary antibody (anti-BTS venom IgG raised in rabbits as described above; 40 μL of 10.0 mg/mL antibody added to PBS-buffered 3% BSA) overnight at RT with constant gentle shaking. The membranes were rinsed 3 × with Tris buffered saline (TBS, 0.05 M Tris-HCl, 0.15 M NaCl, pH 7.4) and then secondary antibody (5 μL goat anti-rabbit IgG conjugated with alkaline phosphatase) in 15 mL TBS was incubated with the membrane for 60 min at RT with gentle shaking. Membranes were then washed 4 × with TBS, and alkaline phosphatase substrate (Roche BCIP/NBT, 5-bromo-4-chloro-3-indolyl-phosphate/Nitrotetrazolium Blue, prepared following the manufacturer's instruction) in 10 mL of MilliQ™ water was added. The color reaction was stopped with 20 mM disodium EDTA in PBS after ~5 min. Membranes were washed in MilliQ™ water, dried and photographed.

2.10. Azocasein metalloproteinase and inhibition by anti-BTS venom antibodies assays

Metalloproteinase activity toward azocasein was assayed using the method of Smith and Mackessy [55] with modifications. Forty μL *B. irregularis* venom was incubated with 1 mg of azocasein substrate in 0.5 mL buffer (50 mM HEPES, 100 mM NaCl, pH 8.0) for 1 h at 37 °C; activity was stopped, and unreacted substrate precipitated, with 0.5 M trichloroacetic acid, and the supernatant was read at 342 nm. Specific activity was expressed as $\Delta A_{342\ nm}$/min/mg venom protein. For inhibition by anti-BTS venom antibody assays, 40 μg of venom was incubated with 1 ×, 10 × or 25 × (by weight) lyophilized IgGs in a total volume of 0.5 mL for 30 min at RT; assays were then conducted as

above. Controls using anti-BTS IgG only were run for each level and subtracted from assay values, and results were reported as % activity remaining (compared to assays with just *B. irregularis* (Guam) venom). Two individual adult venom samples were assayed in duplicate.

2.11. Data accessibility

Transcriptomic data has been submitted to the NCBI Sequence Read Archive (https://www.ncbi.nlm.nih.gov/sra) (Bioproject ID: PRJNA401953; Biosample accession: SAMN07612293; Sequence Read Archive code: SRR6012492). All transcripts that resulted in complete translated venom proteins were submitted to GenBank with accession numbers MF948008-MF948117. All LC-MS/MS. raw and .mzXML data, as well as search engine outputs and the search database, can be found on the Mass Spectrometry Interactive Virtual Environment (MassIVE) at https://massive.ucsd.edu/(accession number: MSV000081130 at http://massive.ucsd.edu/ProteoSAFe/dataset.jsp?task=931c5819f582493e9bfbd176fc87c616), as well as through ProteomeXchange [56,57] at http://www.proteomexchange.org/(accession number PXD006636, at http://proteomecentral.proteomexchange.org/cgi/GetDataset?ID=PXD006636).

3. Results and discussion

3.1. Guam B. irregularis transcriptome

For the *B. irregularis* venom gland library, a total of 53,201,077 paired-end reads were obtained with Illumina sequencing and 40,112,608 of these reads were used for the transcriptome assembly after adapter and quality filtering. Trinity *de novo* assembly produced 134,496 contigs with an average contig length of 1879 bps. The Trinity assembly, completed using the Indonesian *B. irregularis* venom gland transcriptome as a reference, resulted in 70,716 contigs with an average contig length of 910 bps. A total of 66% of paired-end reads had sequence overlap (minimum of 10 bps) that could be merged and used as Extender input. With these merged reads, Extender assembled 617 contigs with an average contig length of 1886 bps. Of the three

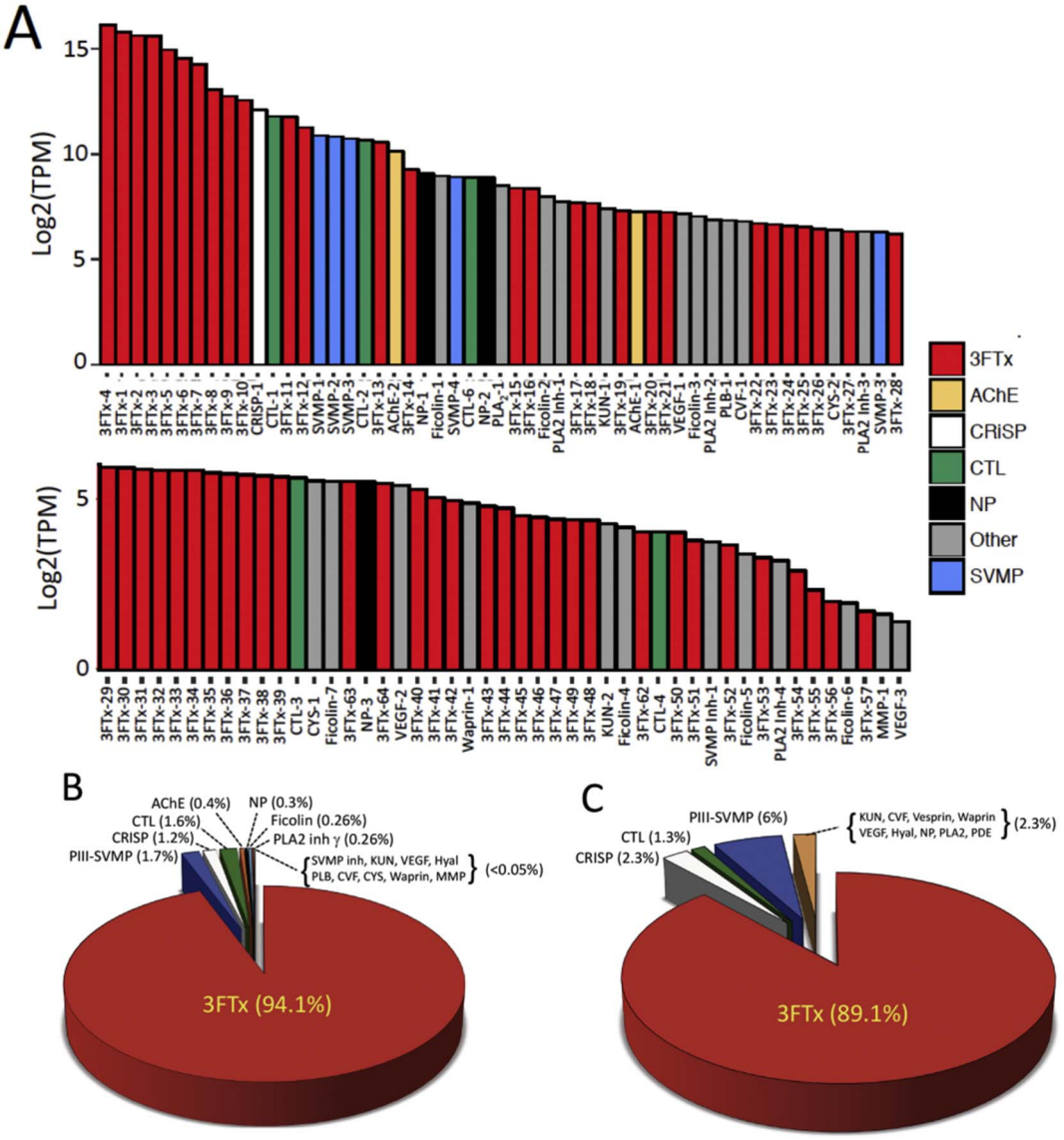

Fig. 1. A) Overview of the 100 most highly transcribed toxin-coding mRNAs in the venom gland of adult Brown Treesnake (*B. irregularis*) from Guam. B) Pie chart of the relative abundances of the toxin families transcribed in the venom gland transcriptome (Table S1). For comparison, the reported composition of Indonesian adult *B. irregularis* venom gland transcriptome [30] is displayed in panel C. Abbreviations: 3FTx, three-finger toxin; CRISP, cysteine-rich secretory protein; CTL, C-type lectin-like; SVMP, snake venom metalloproteinase; AChE, acetylcholinesterase; NP, natriuretic peptide; PLA_2, type IIE phospholipase A_2; PLA_2 Inh, inhibitor of PLA_2; KUN, Kunitz-type protease inhibitor; VEGF, vascular endothelial growth factor; PLB, phospholipase B; CVF, cobra venom factor; CYS, cystatin; SVMP Inh, inhibitor of SVMP; MMP, matrix metalloproteinase. (For interpretation of the references to color in this figure legend, the reader is referred to the web version of this article.)

assemblies, the Trinity genome-guided and Extender assemblies produced the greatest number of full-length translated venom proteins.

Contigs with the highest Transcripts Per Million (TPM) values were identified as partial or complete venom protein sequences (Fig.1). It was discovered that for the top 1000 expressed contigs, those without a BLASTx result still did have a significant BLASTn hit to a venom protein transcript within the nt database, but they were partial transcripts largely consisting of untranslated regions. This demonstrates the limitation of only using BLASTx to identify venom protein transcripts, and it is most likely the reason that previously examined venom gland transcriptomes report a significant percentage (~40%) of unidentified transcripts [36,58,59]. A high abundance of venom protein transcript expression is commonly observed for snake venom glands [35,57,58], especially at four days following venom extraction when there are high levels of venom protein transcript expression [60].

From the final combined transcriptome assemblies, a total of 110 unique full-length translated venom proteins from 18 toxin superfamilies were identified (Fig.1). These venom protein superfamilies include, in order of abundance (Table S1), 65 three-finger toxins (3FTx), 7 metalloproteinases (SVMP), 6C-type lectins (CTL), 1 cysteine-rich secretory proteins (CRISP), 2 acetylcholinesterases (AchE), 3 natriuretic peptides (NP), 7 ficolins, 4 phospholipase A_2 (PLA_2) inhibitors, 2 PLA_2s, 3 vascular endothelial growth factors (VEGF), 2 Kunitz-type protease inhibitors (KUN), 2 cystatins (CYS), 1 phospholipase B (PLB), 1 cobra venom factor (CVF), 1 waprin, 1 SVMP inhibitor, 1 matrix metalloproteinase (MMP), and 1 hyaluronidase (HYAL) (Fig.1, Table S1). A similar result, with 108 unique full-length venom proteins comprising 15 protein superfamilies, was obtained for the Indonesian *B. irregularis* venom gland toxin transcriptome [30]. However, it is subjective to state unequivocally which components are part of the toxin transcriptome for low abundance venom proteins, as transcript levels this low are likely not biologically significant. The Guam *B. irregularis* venom gland toxin transcriptome was largely dominated by 3Ftxs, also consistent with what was previously observed for the Indonesia *B. irregularis* [30]. In this sense, this species appears to have a venom phenotype that is similar to that of many elapids, which often have an abundance of 3FTxs.

Three-finger toxin isoforms were the most abundantly expressed transcripts comprising 94% of all venom protein transcript reads (Fig. 1). Three-finger toxins also exhibited the highest level of isoform diversity, with 65 different isoforms seen at the amino acid level (Table S2); many more isoforms are likely present at the nucleotide level. SVMPs, ficolins, and C-type lectins also exhibited multiple protein isoforms. A greater number of SVMP isoforms were observed for the Indonesian *B. irregularis*, as well as an increase in expression level of SVMP transcripts [30] (Fig. 1C). This was the most distinctive difference between the venom gland transcriptomes of *B. irregularis* originating from the two localities. However, both studies were limited to one snake venom gland transcriptome for each locality, and it has been noted that full characterization of a species representative venom gland transcriptome requires sequencing more than one individual [61]. Because such low variation in venom protein superfamily expression was observed between the two *B. irregularis* localities, it is difficult to conclude that the variation observed is natural or is due to invasive adaptation and dietary change for the Guam *B. irregularis*. Variation in

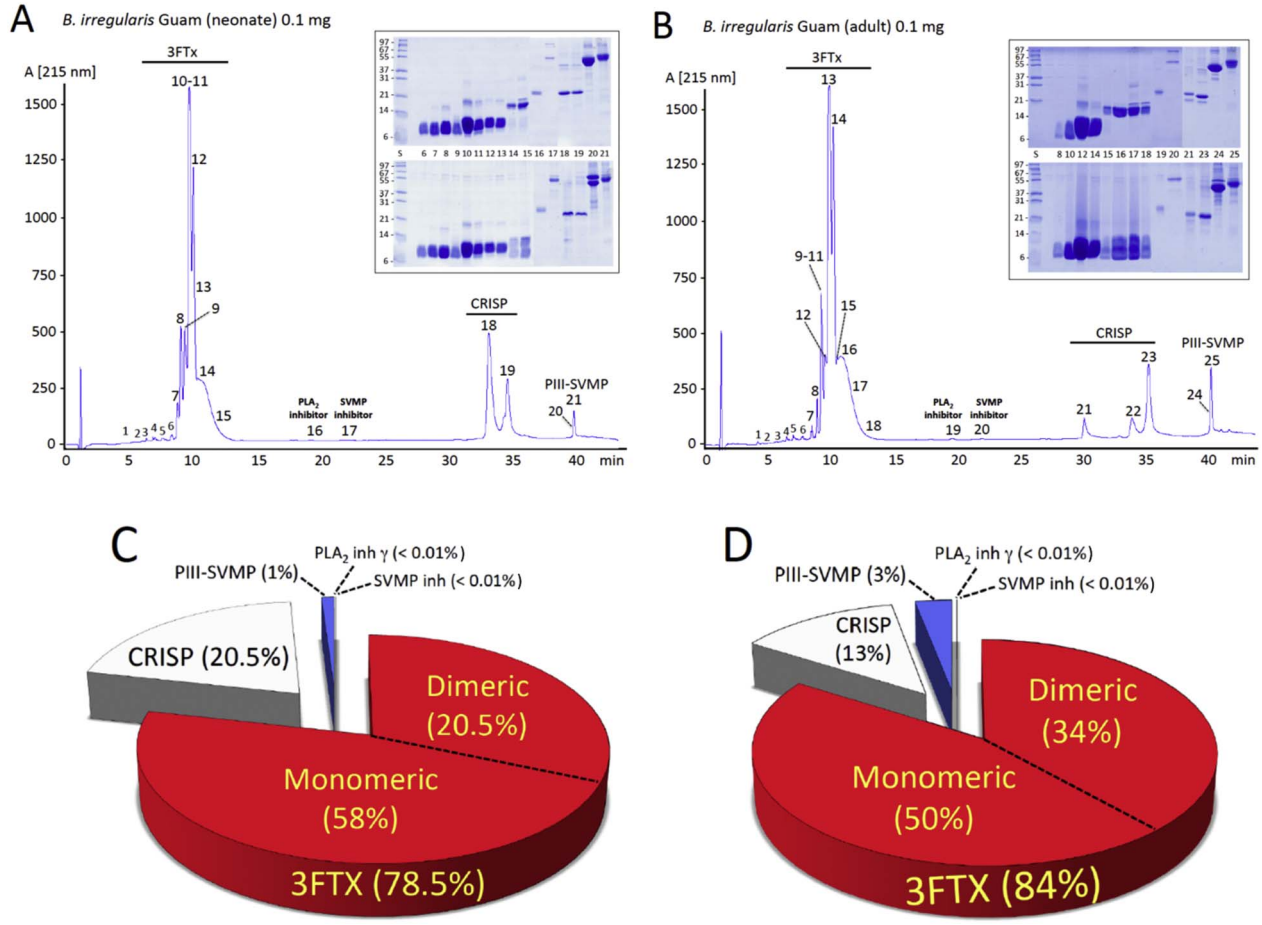

Fig. 2. Reverse-phase chromatographic separations of the proteins of venoms from neonate (A) and adult (B) *B. irregularis* specimens from Guam. Fractions were collected manually and analyzed by SDS-PAGE (insets) under non-reduced (upper panels) and reduced (lower panels) conditions. Protein bands were excised, in-gel digested with trypsin, and identified by bottom-up LC-nESI-MS/MS (Supplementary Table S3). Pie charts in panels C and D display, respectively, the relative occurrence (in percentage of total venom proteins) of toxins from different protein families in the venoms of neonate and adult *B. irregularis* specimens from Guam. Acronyms as in Fig.1.

the expression level of venom protein transcript isoforms and venom protein superfamilies has been reported for *Crotalus adamanteus* from different localities [61]. *Boiga irregularis* also exhibited locality-specific isoforms, with only a single 3FTx isoform shared (with 100% identity) between the two localities (3FTx_03 from Guam and Birre_3FTx-9d from Indonesia).

Transcript 3FTx_01 was found to be identical to NCBI database three-finger toxin 3 (KU666930), 3FTx_06 was identical to database three-finger toxin 1 (KU666929) and 3FTx_46 was identical to database three-finger toxin 5 (KU666932); these transcripts originated from extracellular mRNA within Guam *B. irregularis* venom [62]. With the exception of one amino acid within the signal peptide, 3FTx_02 was found to be identical to database three-finger toxin 6 (KU666933), and a three amino acid difference in the signal peptide between 3FTx_40 and three-finger toxin 4 (KU666931) was also observed. It is likely that these few amino acid differences within the signal peptides are due to the use of a degenerate PCR primer within this region to obtain the sequences of extracellular mRNA transcripts [60]. Therefore, transcripts obtained from the next-generation sequencing (NGS) venom gland tissue transcriptome were found to be identical to those observed within the venom of *B. irregularis*, with one of these transcripts even corresponding to the mature protein sequence of Irditoxin B, highlighting the application of using venom extracellular mRNA to obtain venom protein transcripts of both abundant and novel toxins [62].

As also noted for the Indonesian *B. irregularis* venom gland transcriptome, transcript sequences identical to Irditoxin A and B were not found. Transcripts that shared the greatest identity (96% to subunit A and 97% to subunit B) exhibited at least three amino acid substitutions within the signal peptide region, which would still produce a mature protein that would be identical to each Irditoxin subunit. This lack of transcripts identical to both Irditoxin subunit transcripts, coupled with the fact that only one identical 3FTx isoforms [ANN23940, 3FTx_4] (Table S2) is shared between Indonesian and Guam Brown Treesnakes, demonstrates the rapid nature of amino acid substitution exhibited by *B. irregularis* venom proteins, particularly those that are abundantly expressed within venom glands [63].

3.2. The venom proteomes of neonate and adult B. irregularis from Guam

The venom toxin compositions of neonate and adult Guam Brown Treesnakes were initially assessed through a bottom-up protocol. Venoms were fractionated by reverse-phase (RP) HPLC (Fig. 2, panels A and B), the individual peaks quantified spectrophotometrically (Fig. 2, panels C and D), the RP fractions analyzed by SDS-PAGE, and the electrophoretically resolved protein bands identified *via* a tryptic-peptide-centric MS/MS approach and BLAST analysis [48,49]. *De novo* assigned venom proteins are listed in Table S3. This approach yielded multiple hits to both Guam and Indonesian *B. irregularis* transcripts, providing an overview of venom toxin composition at protein family resolution. The combined RP-HPLC/SDS-PAGE/MS/MS data revealed that the venom proteomes of neonate (N) and adult (A) *B. irregularis* were both overwhelmingly (78 and 84%, respectively) dominated by monomeric and dimeric 3FTxs, followed by moderately abundant (21% (N) and 13% (A)) CRISP molecules, low abundance (1% (N) and 3% (A)) PIII-SVMPs, and very low abundance (< 0.01%) PLA_2 and SVMP inhibitors. Although there is good correlation between the transcriptomic and proteomic abundance of major (3FTx) and some minor (SVMP, SVMP inhibitor) protein families, both datasets clearly depart

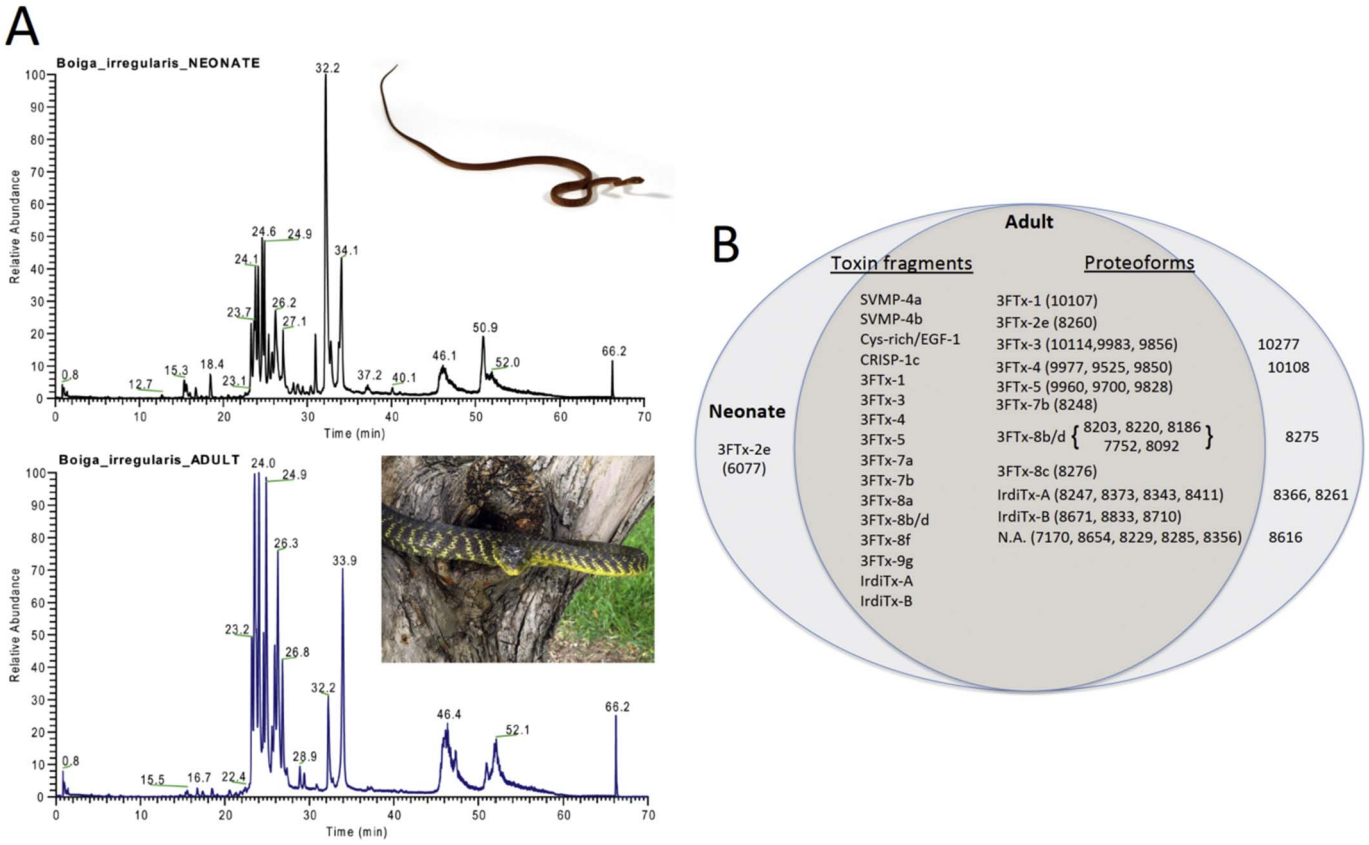

Fig. 3. LC-top-down MS analysis of *B. irregularis* (Guam) neonate and adult venoms. Panel A, total ion current (TIC) profiles of representative reduced venom proteins of neonate (upper panel) and adult (lower panel) *B. irregularis* individuals separated by ultra-high performance liquid chromatography (uHPLC). Downstream top-down MS/MS protein IDs are listed in Tables S4 and S5, respectively. Quantitative ratios from extracted and aligned ion chromatograms are shown in Table S5. Photos of neonate (upper panel) and adult (lower panel) *B. irregularis* (Guam), courtesy of Dr. Shane R. Siers© and Dr. Steve Mackessy©. Panel B, Venn diagram showing the distribution of unique and shared full-length 3FTx proteoforms and toxin fragments among *B. irregularis* (Guam) neonate and adult venoms.

in their overall toxin compositional patterns and, strikingly, also in their CRISP content (compare Fig. 1A and panels C and D of Fig. 2). The reasons for these discrepancies remain elusive, but have been postulated to include i) transient/individual/temporal expression patterns of mRNA expression; ii) post-genomic regulation [64–66]; iii) a "hidden repertoire" of readily translatable transcripts for functional venom adaptation; and iv) methodological or statistical issues [67,68].

The poor resolution of the RP chromatogram section containing 3FTxs (elution time between 9 and 13 min in panels A and B of Fig. 2) did not allow separation of these venom components. High performance liquid chromatography (HPLC) (Fig. 3A) in conjunction with high-resolution top-down MS analysis has the potential for achieving full individual protein characterization [69–72]. This approach enabled the identification of 30 and 25 full-length 3FTxs in the venom proteome of neonate (Table S4) and adult (Table S5) Brown Treesnakes, respectively. In both age classes, these venom toxins are proteoforms of the same 10 3FTxs transcripts (Table S2): 3FTx-1 [ANN23938], 3FTx-2e [JAS04641], 3FTx-3 [ANN23939], 3FTx-4 [ANN23940], 3FTx-5 [ANN23941], 3FTx-7b [JAS04618], 3FTx-8b/d [JAS04612], 3FTx-8c [JAS04613], and the subunits A [A05864] and B [A05865] of Irditoxin [2H7Z] [26]. In addition, 6 and 5 masses in the expected range for 3FTxs (7.1–8.6 kDa) could not be assigned in the neonate and adult venom proteomes, respectively. Further, the occurrence of multiple proteoforms of 3FTxs in both age class venoms, and the fact that 3FTx-2e, 3FTx-7b, 3FTx-8b/d and 3FTx-8c sequences were matched to mRNAs found in the venom gland transcriptome of Indonesian *B. irregularis* [30], highlights the utility of using multiple approaches toward defining snake venom gland proteomes/transcriptomes. On the other hand, the low conservation between the sets of 3FTxs expressed in the venom glands of *B. irregularis* from Guam and Indonesia, as suggested in an earlier MALDI-TOF-MS-based dataset [25], is remarkable. Multiple sequence analysis and cladistic analysis of Guam and Indonesian *B. irregularis* 3FTxs shows three major clades, each grouping proteins from the two geographic congeneric variants (Fig. 4). Each clade contains highly similar 3FTx sequences exhibiting distinctive features. Clade C1 3FTxs have a deletion of a 7-amino- acid stretch (positions ^{27}(R/Q) IGWG(A/K)G^{34}), which is present in the 3FTxs of clades C2 and C3. In addition, C1 3FTxs' dipeptide ^{63}TG^{64} is absent in C2 3FTxs and substituted by ^{63}PP^{64} in the sequences of clade C3 (Fig.4A). This pattern of intraspecific amino acid sequence divergence suggests rapidly evolving 3FTx genes as the cause of the observed geographic variation, consistent with the birth-and-death model of multigene family evolution [73,74].

All 25 3FTx proteoforms and the 5 unassigned masses found in adult *B. irregularis* venom were also identified in the neonate's venom (Fig. 3B). In addition, both venoms shared a number of very low abundance toxin fragments (Fig. 3B) (highlighted in Tables S4 and S5). These fragments mainly eluted within the first 23 min of the chromatographic separation (Fig. 3A) but were also found randomly distributed across the chromatograms. Although the reason for the occurrence of these peptides is puzzling, their presence indicates that, in addition to the intact proteins identified in the neonate and adult venoms, proteins 3FTx-7a [JAS04619], 3FTx-8a [JAS04615], 3FTx-8f [JAS04610], 3FTx-9 g [JAS04603], SVMPs 4a [JAS04560] and 4b [JAS04559], CRISPs 1 [JAG68295] and 1c [JAS04594] were also synthesized in the venom gland of both neonate and adult Guam *B. irregularis*.

Comparison of the 3FTx sequences encoded by full-length mRNAs with the corresponding proteins characterized by top-down MS in the venoms of neonate and adult *B. irregularis* evidenced two modes of post-translational processing operating in the venom gland to produce mature 3FTx molecules. On the one hand, cleavage of a 19-residue signal peptide [MKTLLLALAVVAF(V/M)CLGSA], release of a 15-residue N-terminal extension [DQLGLGR(P/Q)RI(G/D)WGQG], and conversion of N-terminal glutamine to 5-oxopyrrolidine-2-carboxylic acid (pyroglutamate) represented a common mechanism for the biosynthesis of mature 3FTx-3 proteoform-1 (9983.5 Da), 3FTx-8b/d (8203.66 Da, 8204.65 Da) and the A and B subunits of Irditoxin in both neonate and adult venom glands (Tables S4 and S5). Conversely, proteoforms of 3FTxs 1, 3, 4 and 5 acquire their mature form by release of the signal peptide and eventual trimming of one or more N-terminal amino acids. N-terminal modification with pyroglutamate is a common feature of non-conventional 3FTxs from rear-fanged snake venoms [20,26,75,76], and its presence has been suggested to stabilize proteins against proteolytic degradation [77]. However, the functional consequences of alternative 3FTx maturation processing remain elusive.

3.3. Differential translation of venom proteins between neonate and adult *B. irregularis* from Guam

Despite the overlapping sets of venom components expressed in both neonate and adult snakes (Fig. 3), the relative abundances of the

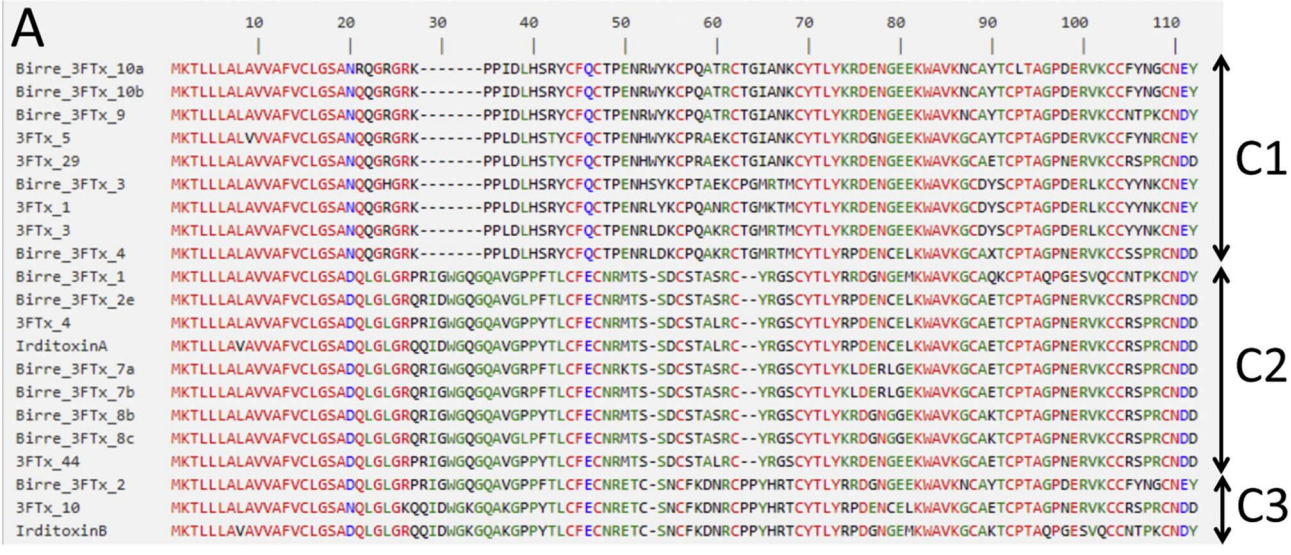

Fig. 4. Multiple sequence alignment (panel A) and neighbor-joining cladistic analysis (panel B) of precursor amino acid sequences of the 3FTx molecules identified in the venoms of Guam and Indonesian *B. irregularis*.

toxins differ between age classes. The most abundant components in the neonate venom proteome are the proteoforms of 3FTx-8b/d (16.1% of the total venom proteome), Irditoxin subunits A (6.5%) and B (7.6%), 3FTx-3 (4.7%), and 3FTx-4 (3%). In the adult venom proteome the most abundant toxins are the proteoforms of Irditoxin chains A (17.1%) and B (13.2%), 3FTx-4 (9.4%), 3FTx-3 (7.4%), 3FTx-8b/d (6.6%), 3FTx-5 (3.9%), and 3FTx-7b (3.0%). A comparative analysis of the relative abundances of toxin proteoforms between *Boiga* age classes is displayed in Table S6. The volcano plot shown in Fig. 5 highlights in red those venom proteins that display both large magnitude fold-changes (points that are far to either the left- or right-hand sides) and higher statistical significance (points that are found toward the top of the plot) between adult and neonate *B. irregularis* specimens from Guam. The biological roles of these differential translation patterns are elusive, demonstrating that a toxicovenomics analysis is necessary [78,79]. However, it seems reasonable to propose that, being an adaptive trophic trait, ontogenetic venom variation likely correlates with differences in prey consumption [80–82]. Brown Treesnakes undergo a pronounced ontogenetic shift in prey preference, from a diet consisting almost exclusively of ectothermic prey (small lizards, particularly *Carlia* skinks and *Hemidactylus* geckos) in neonate snakes, to both ectothermic and endothermic vertebrates (birds and mammals) being consumed by adults [3,7,83]. As documented in other snake species [84,85], these dietary changes in *B. irregularis* are accompanied by a shift in venom composition and taxa-specific toxicity, with neonate snakes producing more toxic venom toward house geckos (*Hemidactylus frenatus*) [25]. Irditoxin, found in both neonate and adult *B. irregularis*, has potent lethal paralytic effects toward both lizards and birds [28]; unraveling the venom components responsible for additional differential effects toward specific prey will greatly facilitate an understanding of the selective mechanisms driving snake venom evolution.

3.4. Antivenomics analysis of rabbit anti-BTS venom IgGs

Non-front-fanged colubroid (NFFC) snakes comprise about two-thirds of the extant ophidian species, and growing evidence indicates that at least one-third of the > 2300 species of NFFC snakes produce venom in a specialized Duvernoy's venom gland [21,86,87]. A number of species are able to deliver lethal quantities of venom and/or cause human envenomings of medical significance (*e.g.*, *Dispholidus typus*, *Thelotornis capensis*, *Rhabdophis tigrinus*, *R. subminiatus*, *Balanophis ceylonensis*, *Philodryas olfersii*, *P. baroni*, *P. chamissonis*, *P. patagoniensis*, *P. viridissima*, *Alsophis portoricensis*, and *Tachymenis peruviana*) [88,89] and references cited therein. The weak neurotoxicity toward mammalian prey [26] suggests that bites by *B. irregularis* are unlikely to cause more than mild to moderate local swelling and pain, and occasionally local bruising, paresthesia/numbness, erythema or bleeding in adult humans [27,28,90]. Symptoms requiring medical attention have been reported in bites to children [31]; however, no antivenom is available and so we have generated a rabbit antiserum and evaluated the immunological profile of caprylic acid-purified IgGs.

Western blot analysis (Fig. 6) showed good reactivity across the full range of *B. irregularis* venom proteins and cross-reactivity towards orthologous toxins, particularly SVMPs, CRISPs, and 3FTxs, from a number of rear-fanged snake venoms, and also from Elapidae (King Cobra, *O. hannah*). Second generation antivenomics [53] was applied to quantitate the reactivity of anti-BTS IgGs towards the venom proteins of neonate and adult homologous taxa (Fig. 7). In both cases, rabbit IgGs immunoretained quantitatively CRISPs and PIII-SVMPs, and 60–70% of 3FTxs. As reported for other antivenoms [89], the apparent low recovery of PIII-SVMPs in the immunoaffinity captured fractions may be ascribed to the high affinity of these venom proteins for antivenom molecules, as evidenced by the strong reactivity of these fractions against the rabbit IgGs by Western blot analysis (Fig. 7, panel A). In addition, incubation with increasing amounts of anti-BTS IgGs impaired, in a concentration-dependent manner, the azocasein SVMP activity of adult *B. irregularis* venom (Fig. 8).

Non-immunoretained adult venom fraction contained a mixture of the most abundant toxins, including 3FTx-8b/d proteoforms (reduced molecular masses 8275.7, 8203.6, 8220.6 Da), Irditoxin chain A (8247.6 Da), 3FTx-7b (8248.5 Da), 3FTx-3 (9983.5 Da), 3FTx-4 (9850.5 and 9978.5 Da), and 3FTx-5 (9829.5 Da). Partial binding of these 3FTx proteins was due to saturation of the immobilized antibody binding sites by 0.2 mg of total venom, because incubation with 50 μg resulted in nearly 100% retention of all 3FTxs, whereas when incubations were increased to 100–150 μg, the non-immunoretained fraction increased proportionally.

4. Concluding remarks

Although significant research continues to examine the composition, biological roles, and pharmacological effects of venoms from the

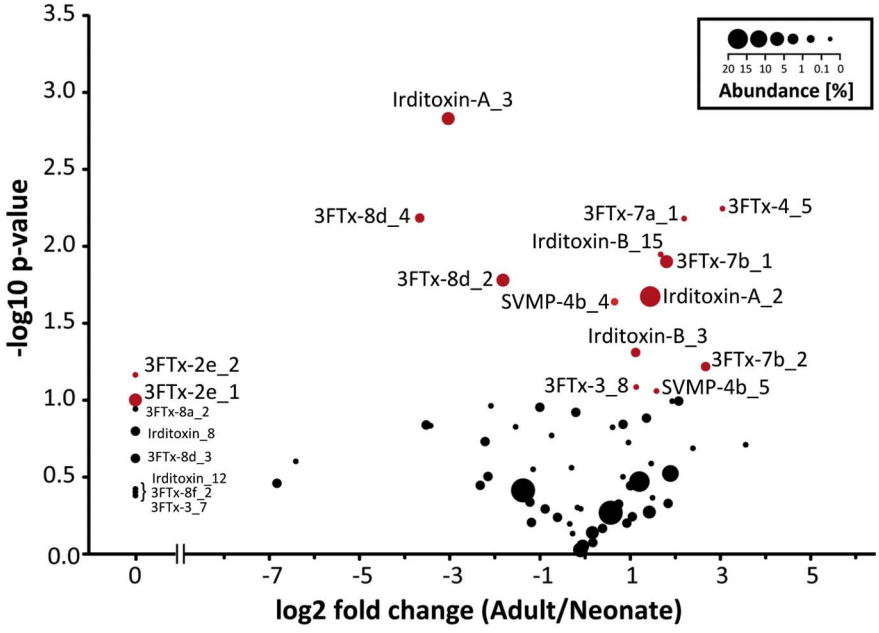

Fig. 5. Volcano plot of adult *vs.* neonate venom toxin abundances (Table S6). The statistical relevance (− log10 of the *p*-value) of the log2 fold change of venom protein abundance between adult and neonate individuals is shown. Each dot represents a proteoform and the size indicates its relative abundance. Red dots highlight significant differentially translated proteins (log2 fold change ≤ − 1.0 or ≥ 1.0 and − log10 of p-value ≥ 1.0). Proteoforms absent in adults are indicated as log2 fold change 0. (For interpretation of the references to color in this figure legend, the reader is referred to the web version of this article.)

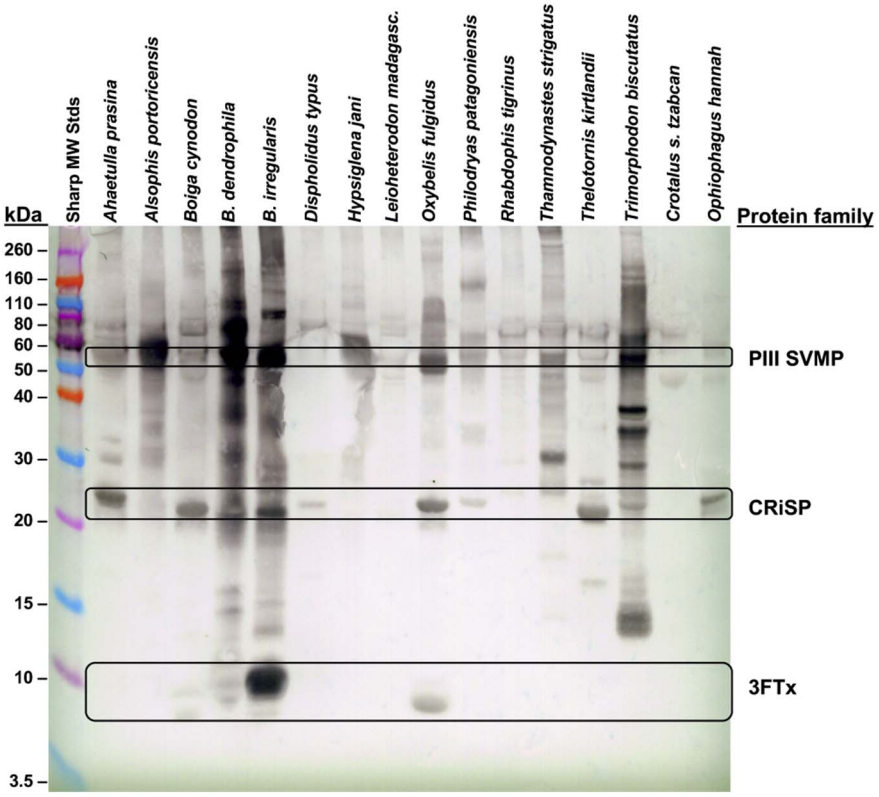

Figure 6. Reactivity of various "colubrid" venoms with *Boiga* venom antibodies. 8 μg venom were run in each lane. Blots were incubated with 40 μL (10 mg/mL) anti-BTS IgGs in 15 mL PBS overnight at room temperature. Blots were developed with goat anti-rabbit labeled with alkaline phosphatase and NBT/BCIP substrate.

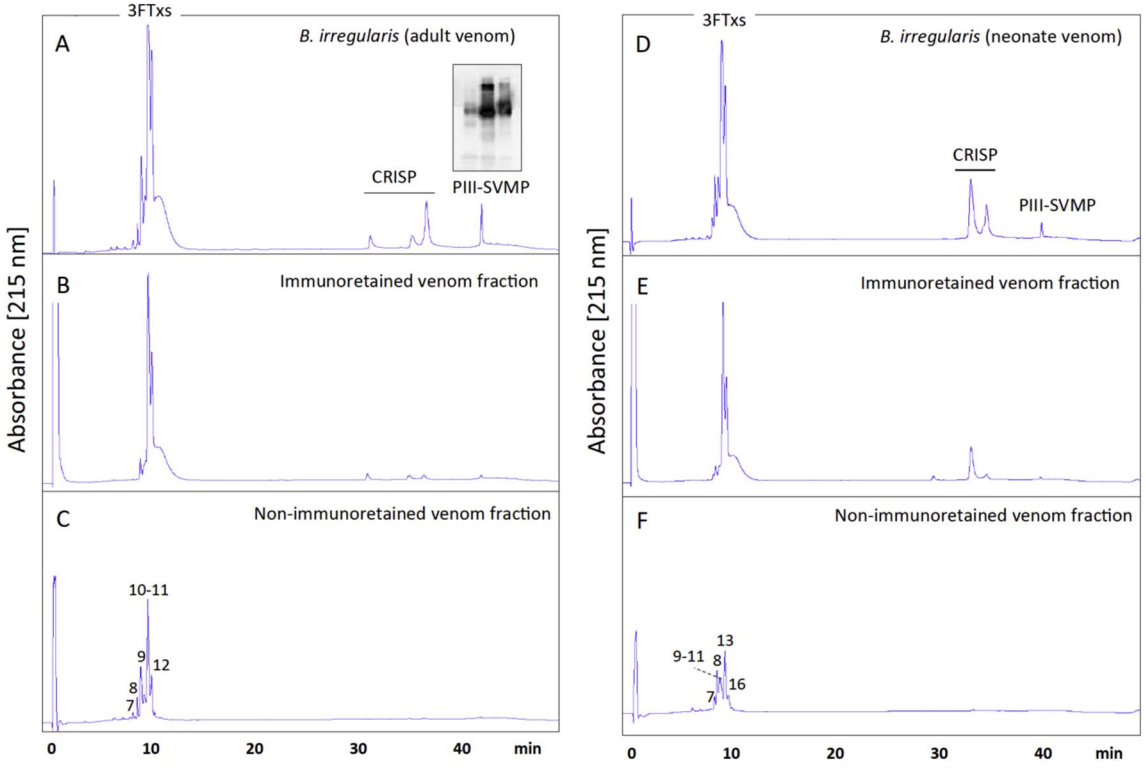

Fig. 7. Immunoaffinity antivenomics analysis of adult (A–C) and neonate (D–F) venom against immobilized anti-BTS venom antibodies. Panels A and D, reference RP-HPLC separation of proteins of adult and neonate venoms, respectively. Protein classes identified in the different chromatographic fractions are highlighted. Panels B and E, and C and F display, respectively, reverse-phase separations of the immunocaptured and the non-bound column fractions recovered after incubation of 100 μg of venom with 300 μL of affinity matrix containing 4.8 mg of immobilized IgGs. Column eluates were monitored at 215 nm and quantified by comparing the areas of homologous peaks in the two fractions.

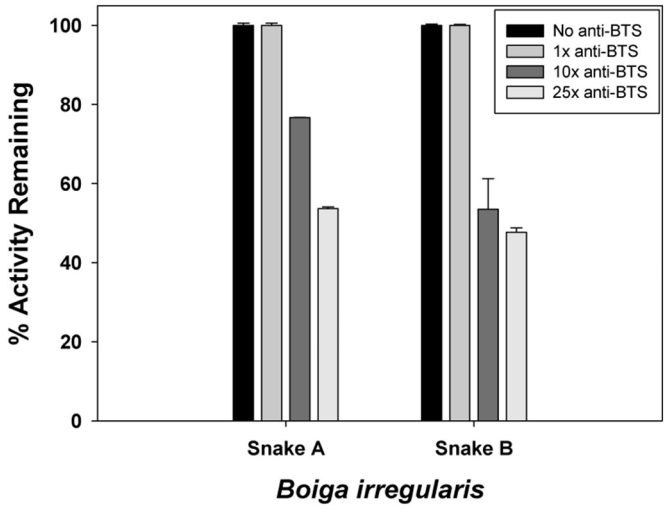

Fig. 8. Azocasein metalloproteinase activity of *B. irregularis* venom in the presence of *Boiga* venom antibodies. Venoms (40 μg; 2 different adult snakes) were incubated in 0.5 mL buffer for 30 min at RT with 0, 10 or 25 times mass amounts of antibodies prior to assays. Values are means ± SD.

truly venomous front-fanged elapid and viperid snakes, rear-fanged snake venoms remain a largely untapped area of venom research. Bottom-up and top-down venomics, as well as venom gland transcriptomics, revealed that the venom proteomes of both neonate and adult Guam *B. irregularis* show a high degree of conservation and overall simplicity in dominant protein family diversity, though differences in toxin abundance are apparent. As trophic traits, these differences are likely driven by prey preference, as neonates consume primarily ectothermic prey, whereas adults take both ectothermic and endothermic prey items. However, neonate *B. irregularis* venom had a significantly lower LD_{50} (18.0 μg/g) towards lab mice (*Mus musculus*) when compared to adult *B. irregularis* venom (31.0 μg/g) [25]. For adult *B. irregularis*, the lack of toxic venom components targeting mammalian prey, as evidenced by previous LD_{50} studies [25], may be due to the use of multiple predatory modalities to subdue prey; envenomation is used to subdue bird and lizard prey, whereas constriction is used to manipulate and subdue mammalian prey [25]. After hatching, a Brown Treesnake undergoes over a 600% increase in length and a 400-fold increase in mass as an adult [15], and during its growth, the snake also shows a pronounced ontogenetic shift from a diet consisting almost exclusively of ectothermic prey (small lizards) to mainly endotherms (birds and mammals) as adults [3,7,85]. Undoubtedly, the consumption of larger mammalian prey by adult *B. irregularis* is significantly more metabolically favorable than consuming smaller ectothermic prey, but the possibility that this predatory strategy, constriction, is driving variation in venom composition remains to be explored. Further, to determine whether the ontogenetic venom shift is truly functionally related to the trophic shift, represents an epiphenomenon, or a neutral trait contingent on other developmental factors, requires further detailed data on the toxicity of the adult and juvenile venoms toward natural prey.

Bites to humans from *B. irregularis* on Guam do occur, often when the person is sleeping, and it has been estimated that 1 in 1200 emergency room visitors seek treatment for bites [31]. Although these bites are not life-threatening, the potential for injury, especially to young children, is possible. Our antivenomic analyses reveal that the rabbit anti-BTS venom IgGs are effective at immunocapturing the majority of neonate and adult *B. irregularis* venom compounds. Interestingly, these IgGs also demonstrated strong immunoreactivity (by Western blot analysis) toward PIII-SVMPs in the venoms of *B. dendrophilia*, *Alsophis portoricensis*, and *Trimorphodon biscutatus*, suggesting a conservative immunoreactive epitope across PIII-SVMPs of these species. Conversely, although 3FTxs in *B. irregularis* venoms showed strong immunoreactivity with anti-BTS IgGs, those in several other rear-fanged snake venoms, and in venom of the elapid *Ophiophagus*, did not cross-react, indicating that epitopes in these diverse yet structurally conservative molecules are quite distinct.

A limitation of our work is the small number of specimens sampled. The inferences of our work may be to a certain extent affected by the well-documented occurrence of intraspecific individual and geographic variability of snake venoms [85,91]. In particular, elucidating the temporal sequence of the ontogenetic changes experienced by the venom of *B. irregularis* ideally requires performing detailed venomic analyses of multiple individuals from birth to adulthood [92]. On the other hand, analyses using genetic markers from 65 *B. irregularis* specimens from different geographical locations across its native and introduced ranges show significant phylogeographic structure, with the northernmost sampled population of *B. irregularis* from Pulau Tahulandang, Sulawesi (Indonesia) forming the sister group to all remaining lineages within *B. irregularis* [12]. The presence of genetic structure among different populations of *B. irregularis* suggests that the differences in venom composition noted here may have resulted from a rapid, insular-type pattern of divergence associated with incipient allopatric differentiation/speciation [93,94]. However, testing this hypothesis would require analysis of the proteome/transcriptome of numerous populations of *B. irregularis* and is far beyond the scope of the present study.

Supplementary data to this article can be found online at https://doi.org/10.1016/j.jprot.2017.12.020.

Transparency document

The http://dx.doi.org/10.1016/j.jprot.2017.12.020 associated with this article can be found, in online version.

Acknowledgements

This study was supported by grants BFU2013-42833-P (Ministerio de Economía y Competitividad, Madrid, Spain) to JJC, and PE 2600/1 (Deutsche Forschungsgemeinschaft, Bonn, Germany) to DP. The research was funded by a *Major Research Instrumentation* grant, *MRI*-1429003: Acquisition of a High Performance Computing Cluster for Multidisciplinary Research and Education at the University of Northern Colorado to SF. The authors thank Dr. Shane R. Shiers (http://www.macronesia.net/about/) (USDA-APHIS, Wildlife Services National Wildlife Research Center, Hilo, Hawaii, USA) for the picture of neonate *B. irregularis* shown in Fig. 3 and the Graphical Abstract.

References

[1] J.M. Bechstein, Herrn de Lacépède's Naturgeschichte der Amphibien oder der eyerlegenden vierfüssigen Thiere und der Schlangen. Eine Fortsetzung von Buffon's Naturgeschichte, Weimar: Verlage des Industrie Comptoir's (1800–1802) 1–524 http://biodiversitylibrary.org/bibliography/5009#/summary.

[2] G.H. Rodda, T.H. Fritts, M.J. McCoid, E.W. Campbell III, An overview of the biology of the Brown Treesnake (*Boiga irregularis*), a costly introduced pest on Pacific islands, in: G.H. Rodda, Y. Sawai, D. Chiszar, H. Tanaka (Eds.), Problem Snake Management: The Habu and the Brown Treesnake, Cornell University Press, Ithaca, NY, 1999, pp. 44–80 (available from), http://digitalcommons.unl.edu/icwdm_usdanwrc/659.

[3] H.W. Greene, Ecological, evolutionary, and conservation implications of feeding biology in old world cat snakes, genus *Boiga* (Colubridae), Proc. Calif. Acad. Sci. 46 (1989) 193–207.

[4] G.H. Rodda, T.H. Fritts, P.J. Conry, Origin and population growth of the brown tree snake, *Boiga irregularis*, on Guam, Pac. Sci. 46 (1992) 46–57.

[5] J.N. Caudell, M.R. Conover, J. Whittier, Predation of Brown Treesnakes (*Boiga irregularis*) in Australia, Intl. Biodet. Biodegrad. 49 (2002) 107–111.

[6] J.A. Savidge, Extinction of an island forest avifauna by an introduced snake, Ecology 68 (1987) 660–668.

[7] J.A. Savidge, Food habits of *Boiga irregularis*, an introduced predator on Guam, J. Herpetol. 22 (1988) 275–282.

[8] G.H. Rodda, T.H. Fritts, The impact of the introduction of the colubrid snake *Boiga irregularis* on Guam's lizards, J. Herpetol. 26 (1992) 166–174.

[9] T.H. Fritts, G.H. Rodda, The role of introduced species in the degradation of island ecosystems: a case history of Guam, Ann. Rev. Ecol. Systemat. 29 (1998) 113–140.
[10] G.J. Wiles, J. Bart, R.E. Beck Jr., C.F. Aguon, Impacts of the Brown Treesnake: patterns of decline and species persistence in Guam's avifauna, Conserv. Biol. 17 (2003) 1350–1360.
[11] G. Perry, V. Dice, Forecasting the risk of brown tree snake dispersal from Guam: a mixed transport-establishment model, Conserv. Biol. 23 (2009) 992–1000.
[12] J.Q. Richmond, D.A. Wood, J.W. Stanford, R.N. Fisher, Testing for multiple invasion routes and source populations for the invasive Brown Treesnake (*Boiga irregularis*) on Guam: implications for pest management, Biol. Invasions 17 (2015) 337–349.
[13] H.S. Mortensen, Y.L. Dupont, Snake in paradise: disturbance of plant reproduction following extirpation of bird flower-visitors on Guam, Biol. Conserv. 141 (2008) 2146–2154.
[14] G.H. Rodda, T.H. Fritts, D. Chiszar, The disappearance of Guam's wildlife, Bioscience 47 (1997) 565–575.
[15] S.R. Siers, J.A. Savidge, R.N. Reed, Quantile regression of microgeographic variation in population characteristics of an invasive vertebrate predator, PLoS One 12 (2017) e0177671.
[16] I.T. Moore, M.G. Greene, Physiological evidence for reproductive suppression in the introduced population of brown tree snakes (*Boiga irregularis*) on Guam, Biol. Conserv. 121 (2005) 91–98.
[17] H.S. Rogers, E.R. Buhle, J. HilleRisLambers, E.C. Fricke, R.H. Miller, J.J. Tewksbury, Effects of an invasive predator cascade to plants via mutualism disruption, Nat. Commun. 8 (2017) 14557.
[18] E.M. Caves, S.B. Jennings, J. Hillerislambers, J.J. Tewksbury, H.S. Rogers, Natural experiment demonstrates that bird loss leads to cessation of dispersal of native seeds from intact to degraded forests, PLoS One 8 (2013) e65618.
[19] T.H. Fritts, D. Leasman-Tanner, The Brown Treesnake on Guam: How the Arrival of one Invasive Species Damaged the Ecology, Commerce, Electrical Systems and Human Health on Guam: A Comprehensive information source. Information and Technology Report 2002–0009, U.S. Geological Survey Publications Warehouse, 2001.
[20] S.P. Mackessy, Biochemistry and pharmacology of colubrid snake venoms, J. Toxicol. Toxin Rev. 21 (2002) 43–83.
[21] A.J. Saviola, M.E. Peichoto, S.P. Mackessy, Rear-fanged snake venoms: an untapped source of novel compounds and potential drug leads, Toxin Rev. 33 (2014) 185–201.
[22] S.R. Levinson, M.H. Evans, F. Groves, A neurotoxic component of the venom from Blanding's treesnake (*Boiga blandingi*), Toxicon 14 (1976) 307–312.
[23] M. Broaders, C. Faro, M.F. Ryan, Partial purification of acetylcholine receptor binding components from the Duvernoy's secretions of Blanding's treesnake (*Boiga blandigi*) and the mangrove snake (*Boiga dendrophila*), J. Nat. Toxins 8 (1999) 155–165.
[24] N.G. Lumsden, B.G. Fry, S. Ventura, R.M. Kini, W.C. Hodgson, Pharmacological characterisation of a neurotoxin from the venom of *Boiga dendrophila* (mangrove catsnake), Toxicon 45 (2005) 329–334.
[25] S.P. Mackessy, N.M. Sixberry, W.H. Heyborne, T. Fritts, Venom of the brown treesnake, *Boiga irregularis*: ontogenetic shifts and taxa-specific toxicity, Toxicon 47 (2006) 537–548.
[26] J. Pawlak, S.P. Mackessy, N.M. Sixberry, E.A. Stura, M.H. Le Du, R. Ménez, C.S. Foo, A. Ménez, S. Nirthanan, R.M. Kini, Irditoxin, a novel covalently linked heterodimeric three-finger toxin with high taxon-specific neurotoxicity, FASEB J. 23 (2009) 534–545.
[27] D.K. Vest, S.P. Mackessy, K.V. Kardong, The unique Duvernoy's secretion of the Brown Treesnakes (*Boiga irregularis*), Toxicon 29 (1991) 532–535.
[28] S.A. Weinstein, D. Chiszar, R.C. Bell, L.A. Smith, Lethal potency and fractionation of Duvernoy's secretion from the Brown Treesnake, *Boiga irregularis*, Toxicon 29 (1991) 401–407.
[29] S.A. Weinstein, B.G. Stiles, M.J. McCoid, L.A. Smith, K.V. Kardong, Variation of lethal potencies and acetylcholine receptor binding activity of Duvernoy's secretions from the Brown Treesnake, *Boiga irregularis*, J. Nat. Toxins 2 (1993) 187–198.
[30] J.J. McGivern, K.P. Wray, M.J. Margres, M.E. Couch, S.P. Mackessy, D.R. Rokyta, RNA-seq and high-definition mass spectrometry reveal the complex and divergent venoms of two rear-fanged colubrid snakes, BMC Genomics 15 (2014) 1061.
[31] T.H. Fritts, M.J. McCoid, R.L. Haddock, Risks to infants on Guam from bites of the brown treesnake (*Boiga irregularis*), Am. J. Trop. Med. Hyg. 42 (1990) 607–611.
[32] A. Chiszar, Behavior of the brown treesnake, *Boiga irregularis*. A study in applied comparative psychology, in: D. Dewsbury (Ed.), Contemporary Issues in Comparative Psychology, Sinauer, Sunderland, Massachussets, 1990, pp. 101–123.
[33] R.E. Hill, S.P. Mackessy, Venom yields from several species of colubrid snakes and differential effects of ketamine, Toxicon 35 (1997) 671–678.
[34] A.M. Bolger, M. Lohse, B. Usadel, Trimmomatic: a flexible trimmer for illumina sequence data, Bioinformatics (Oxford, England) 30 (2014) 2114–2120.
[35] M.G. Grabherr, B.J. Haas, M. Yassour, J.Z. Levin, D.A. Thompson, I. Amit, X. Adiconis, L. Fan, R. Raychowdhury, Q. Zeng, Z. Chen, E. Mauceli, N. Hacohen, A. Gnirke, N. Rhind, F. di Palma, B.W. Birren, C. Nusbaum, K. Lindblad-Toh, N. Friedman, A. Regev, Full-length transcriptome assembly from RNA-Seq data without a reference genome, Nat. Biotechnol. 29 (2011) 644–652.
[36] D.R. Rokyta, A.R. Lemmon, M.J. Margres, K. Aronow, The venom-gland transcriptome of the eastern diamondback rattlesnake (*Crotalus adamanteus*), BMC Genomics 13 (2012) 312.
[37] J. Zhang, K. Kobert, T. Floury, A. Stamatakis, PEAR: a fast and accurate illumina paired-end reAd mergeR, Bioinformatics (Oxford, England) 30 (5) (2014) 614–620.
[38] B. Langmead, S.L. Salzberg, Fast gapped-read alignment with bowtie 2, Nat. Methods 9 (2012) 357–359.
[39] C. Camacho, G. Coulouris, V. Avagyan, N. Ma, J. Papadopoulos, K. Bealer, T.L. Madden, BLAST +: architecture and applications, BMC Bioinformatics 10 (2009) 421.
[40] F.J. Vonk, N.R. Casewell, C.V. Henkel, A.M. Heimberg, H.J. Jansen, R.J. McCleary, H.M. Kerkkamp, R.A. Vos, I. Guerreiro, J.J. Calvete, W. Wuster, A.E. Woods, J.M. Logan, R.A. Harrison, T.A. Castoe, A.P. de Koning, D.D. Pollock, M. Yandell, D. Calderon, C. Renjifo, R.B. Currier, D. Salgado, D. Pla, L. Sanz, A.S. Hyder, J.M. Ribeiro, J.W. Arntzen, G.E. van den Thillart, M. Boetzer, W. Pirovano, R.P. Dirks, H.P. Spaink, D. Duboule, E. McGlinn, R.M. Kini, M.K. Richardson, The king cobra genome reveals dynamic gene evolution and adaptation in the snake venom system, Proc. Natl. Acad. Sci. U. S. A. 110 (2013) 20651–20656.
[41] T.A. Castoe, A.P.J. de Koning, K.T. Hall, D.C. Card, D.R. Schield, M.K. Fujita, R.P. Ruggiero, J.F. Degner, J.M. Daza, G. Wanjun, J. Reyes-Velasco, K.J. Shaney, J.M. Castoe, S.E. Fox, A.W. Poole, D. Polanco, J. Dobry, M.W. Vandewege, L. Qing, R.K. Schott, The Burmese python genome reveals the molecular basis for extreme adaptation in snakes, Proc. Natl. Acad. Sci. U. S. A. 110 (2013) 20645–20650.
[42] S.F. Altschul, W. Gish, W. Miller, E.W. Myers, D.J. Lipman, Basic local alignment search tool, J. Mol. Biol. 215 (1990) 403–410.
[43] X.J. Min, G. Butler, R. Storms, A. Tsang, OrfPredictor: predicting protein-coding regions in EST-derived sequences, Nucleic Acids Res. 33 (2005) W677–W680.
[44] W. Li, A. Godzik, Cd-hit: a fast program for clustering and comparing large sets of protein or nucleotide sequences, Bioinformatics 22 (2006) 1658–1659.
[45] L. Fu, B. Niu, Z. Zhu, S. Wu, W. Li, CD-HIT: accelerated for clustering the next-generation sequencing data, Bioinformatics 28 (2012) 3150–3152.
[46] B. Li, C.N. Dewey, RSEM: accurate transcript quantification from RNA-Seq data with or without a reference genome, BMC Bioinformatics 12 (2011) 323.
[47] J.J. Calvete, Proteomic tools against the neglected pathology of snake bite envenoming, Exp. Rev. Proteomics 8 (2011) 739–758.
[48] J.J. Calvete, Next-generation snake venomics: protein-locus resolution through venom proteome decomplexation, Exp. Rev. Proteomics 11 (2014) 315–329.
[49] S. Eichberg, L. Sanz, J.J. Calvete, D. Pla, Constructing comprehensive venom proteome reference maps for integrative venomics, Exp. Rev. Proteomics 12 (2015) 557–573.
[50] Q. Kou, L. Xun, X. Liu, TopPIC: a software tool for top-down mass spectrometry-based proteoform identification and characterization, Bioinformatics 32 (2016) 3495–3497.
[51] K. Tamura, G. Stecher, D. Peterson, A. Filipski, S. Kumar, MEGA6: molecular evolutionary genetics analysis version 6.0, Mol. Biol. Evol. 30 (2013) 2725–2729.
[52] G. Rojas, J.M. Jiménez, J.M. Gutiérrez, Caprylic acid fractionation of hyperimmune horse plasma: description of a simple procedure for antivenom production, Toxicon 32 (1994) 351–363.
[53] D. Pla, J.M. Gutiérrez, J.J. Calvete, Second generation snake antivenomics: comparing immunoaffinity and immunodepletion protocols, Toxicon 60 (2012) 688–699.
[54] A.J. Saviola, D. Pla, L. Sanz, T.A. Castoe, J.J. Calvete, S.P. Mackessy, Comparative venomics of the prairie rattlesnake (*Crotalus viridis viridis*) from Colorado: identification of a novel pattern of ontogenetic changes in venom composition and assessment of the immunoreactivity of the commercial antivenom CroFab®, J. Proteomics 121 (2015) 28–43.
[55] C.F. Smith, S.P. Mackessy, The effects of hybridization on divergent venom phenotypes: characterization of venom from *Crotalus scutulatus scutulatus* × *Crotalus oreganus helleri* hybrids, Toxicon 120 (2016) 110–123.
[56] J.A. Vizcaíno, A. Csordas, N. del -Toro, J.A. Dianes, J. Griss, I. Lavidas, G. Mayer, Y. Pérez-Riverol, F. Reisinger, T. Ternent, Q.W. Xu, R. Wang, H. Hermjakob, 2016 update of the PRIDE database and related tools, Nucleic Acids Res. 44 (2016) D447–D456.
[57] J.A. Vizcaíno, E.W. Deutsch, R. Wang, A. Csordas, F. Reisinger, D. Ríos, J.A. Dianes, Z. Sun, T. Farrah, N. Bandeira, P.A. Binz, I. Xenarios, M. Eisenacher, G. Mayer, L. Gatto, A. Campos, R.J. Chalkley, H.J. Kraus, J.P. Albar, S. Martinez-Bartolomé, R. Apweiler, G.S. Omenn, L. Martens, A.R. Jones, H. Hermjakob, ProteomeXchange provides globally co-ordinated proteomics data submission and dissemination, Nat. Biotechnol. 30 (2014) 223–226.
[58] M. Margres, K. Aronow, J. Loyacano, D. Rokyta, The venom-gland transcriptome of the eastern coral snake (*Micrurus fulvius*) reveals high venom complexity in the intragenomic evolution of venoms, BMC Genomics 14 (2013) 1–18.
[59] D.R. Rokyta, K.P. Wray, A.R. Lemmon, E.M. Lemmon, S.B. Caudle, A high-throughput venom-gland transcriptome for the eastern diamondback rattlesnake (*Crotalus adamanteus*) and evidence for pervasive positive selection across toxin classes, Toxicon 57 (2012) 657–671.
[60] D. Rotenberg, E.S. Bamberger, E. Kochva, Studies on ribonucleic acid synthesis in the venom glands of *Vipera palaestinae* (Ophidia, Reptilia), J. Biochem. 121 (1971) 609–612.
[61] D.R. Rokyta, M.J. Margres, M.J. Ward, E.E. Sanchez, The genetics of venom ontogeny in the eastern diamondback rattlesnake (*Crotalus adamanteus*), PeerJ 5 (2017) e3249.
[62] C.M. Modahl, S.P. Mackessy, Full-length venom protein cDNA sequences from venom-derived mRNA: exploring compositional variation and adaptive multigene evolution, PLoS Negl. Trop. Dis. 10 (2016) e0004587.
[63] S.D. Aird, S. Aggarwal, A. Villar-Briones, M.M.-Y. Tin, K. Terada, A.S. Mikheyev, Snake venoms are integrated systems, but abundant venom proteins evolve more rapidly, BMC Genomics 16 (2015) 647.
[64] N.R. Casewell, S.C. Wagstaff, W. Wüster, D.A. Cook, F.M. Bolton, S.I. King, D. Pla, L. Sanz, J.J. Calvete, R.A. Harrison, Medically important differences in snake venom composition are dictated by distinct postgenomic mechanisms, Proc. Natl. Acad. Sci. U. S. A. 111 (2014) 9205–9210.
[65] J. Durban, A. Pérez, L. Sanz, A. Gómez, F. Bonilla, S. Rodríguez, D. Chacón, M. Sasa, Y. Angulo, J.M. Gutiérrez, J.J. Calvete, Integrated "omics" profiling indicates that

miRNAs are modulators of the ontogenetic venom composition shift in the Central American rattlesnake, *Crotalus simus simus*, BMC Genomics 14 (2013) 234.
[66] J. Durban, L. Sanz, D. Trevisan-Silva, E. Neri-Castro, A. Alagón, J.J. Calvete, Integrated venomics and venom gland transcriptome analysis of juvenile and adult Mexican rattlesnakes *Crotalus simus*, *C. tzabcan*, and *C. culminatus* revealed miRNA-modulated ontogenetic shifts, J. Proteome Res. 16 (2017) 3370–3390.
[67] J.J. Li, M.D. Biggin, Gene expression. Statistics requantitates the central dogma, Science 347 (2015) 1066–1067.
[68] D.R. Rokyta, M.J. Margres, K. Calvin, Post-transcriptional mechanisms contribute little to phenotypic variation in snake venoms, G3 5 (2015) 2375–2382.
[69] D. Petras, P. Heiss, R.D. Süssmuth, J.J. Calvete, Venom proteomics of Indonesian king cobra, *Ophiophagus hannah*: integrating top-down and bottom-up approaches, J. Proteome Res. 14 (2015) 2539–2556.
[70] R.D. Melani, O.S. Skinner, L. Fornelli, G.B. Domont, P.D. Compton, N.L. Kelleher, Mapping proteoforms and protein complexes from king cobra venom using both denaturing and native top-down proteomics, Mol. Cell. Proteomics 15 (2016) 2423–2434.
[71] D. Petras, P. Heiss, R.A. Harrison, S.D. Süssmuth, J.J. Calvete, Top-down venomics of the East African green mamba, *Dendroaspis angusticeps*, and the black mamba, *Dendroaspis polylepis*, highlight the complexity of their toxin arsenals, J. Proteomics 146 (2016) 148–164.
[72] S. Ainsworth, D. Petras, M. Engmark, R.D. Süssmuth, G. Whiteley, L.O. Albulescu, T.D. Kazandjian, S. Wagstaff, P. Rowley, W. Wüster, P.C. Dorrestein, A.S. Arias, J.M. Gutiérrez, R.A. Harrison, N.R. Casewell, J.J. Calvete, The medical threat of mamba envenoming in sub-Saharan Africa revealed by genus-wide analysis of venom composition, toxicity and antivenomics profiling of available antivenoms, J. Proteomics (2017), http://dx.doi.org/10.1016/j.jprot.2017.08.016 (Epub ahead of print).
[73] N.M. Ney, A.P. Rooney, Concerted and birth-and-death evolution of multigene families, Annu. Rev. Genet. 39 (2005) 121–152.
[74] B.G. Fry, W. Wüster, R.M. Kini, V. Brusic, A. Khan, D. Venkataraman, A.P. Rooney, Molecular evolution and phylogeny of elapid snake venom three-finger toxins, J. Mol. Evol. 57 (2003) 110–129.
[75] J. Pawlak, S.P. Mackessy, B.G. Fry, M. Bhatia, G. Mourier, C. Fruchart-Gaillard, D. Servent, R. Ménez, E. Stura, A. Ménez, R.M. Kini, Denmotoxin: a three-finger toxin from colubrid snake *Boiga dendrophila* (mangrove catsnake) with bird-specific activity, J. Biol. Chem. 281 (2006) 29030–29041.
[76] W.H. Heyborne, S.P. Mackessy, Isolation and characterization of a taxon-specific three-finger toxin from the venom of the green vinesnake (*Oxybelis fulgidus*; family Colubridae), Biochimie 95 (2013) 1923–1932.
[77] R. Rink, A. Arkema-Meter, I. Baudoin, E. Post, A. Kuipers, S.A. Nelemans, M.H. Akanbi, G.N. Moll, To protect peptide pharmaceuticals against peptidases, J. Pharmacol. Toxicol. Methods 61 (2010) 210-208.
[78] L.P. Lauridsen, A.H. Laustsen, B. Lomonte, J.M. Gutiérrez, Toxicovenomics and antivenom profiling of the eastern green mamba snake (*Dendroaspis angusticeps*), J. Proteomics 136 (2016) 248–261.
[79] L.P. Lauridsen, A.H. Laustsen, B. Lomonte, J.M. Gutiérrez, Exploring the venom of the forest cobra snake: toxicovenomics and antivenom profiling of *Naja melanoleuca*, J. Proteomics 150 (2017) 98–108.
[80] J.C. Daltry, W. Wüster, R.S. Thorpe, Diet and snake venom evolution, Nature 379 (1996) 537–540.
[81] N.J. Da Silva, S.D. Aird, Prey specificity, comparative lethality and compositional differences of coral snake venoms, Comp. Biochem. Physiol. Part C 128 (2001) 425–456.
[82] A. Barlow, C.E. Pook, R.A. Harrison, W. Wüster, Coevolution of diet and prey-specific venom activity supports the role of selection in snake venom evolution, Proc. R. Soc. B 276 (2009) 2443–2449.
[83] B.J. Lardner, J.A. Savidge, G.H. Rodda, R.N. Reed, Prey preferences and prey acceptance in juvenile brown treesnakes (*Boiga irregularis*), Herpetol. Conserv. Biol. 4 (2009) 313–323.
[84] S.P. Mackessy, K. Williams, K.G. Ashton, Ontogenetic variation in venom composition and diet of *Crotalus oreganus concolor*: a case of venom paedomorphosis? Copeia (2003) 769–782.
[85] J.J. Calvete, Venomics: integrative venom proteomics and beyond, Biochem. J. 474 (2017) 611–634.
[86] I.L. Junqueira-de-Azevedo, P.F. Campos, A.T. Ching, S.P. Mackessy, Colubrid venom composition: an -omics perspective, Toxins 8 (2016) E230.
[87] S.P. Mackessy, A.J. Saviola, Understanding biological roles of venoms among the caenophidia: the importance of rear-fanged snakes, Integr. Comp. Biol. 56 (2016) 1004–1021.
[88] S.A. Weinstein, J. White, D.E. Keyler, D.A. Warrell, Non-front-fanged colubroid snakes: a current evidence-based analysis of medical significance, Toxicon 69 (2013) 103–113.
[89] D. Pla, L. Sanz, G. Whiteley, S.C. Wagstaff, R.A. Harrison, N.R. Casewell, J.J. Calvete, What killed Karl Patterson Schmidt? Combined venom gland transcriptomic, venomic and antivenomic analysis of the South African green tree snake (the boomslang), *Dispholidus typus*, Biochim. Biophys. Acta 186 (2017) 814–823.
[90] Clinical Toxinology Resources Website, Toxinology Department, Women's & Children's hospital (WCH), Adelaide, Australia, http://www.toxinology.com/fusebox.cfm?fuseaction=main.snakes.display&id=SN0607.
[91] J.-P. Chippeaux, V. Williams, J. White, Snake venom variability: methods of study, results and interpretation, Toxicon 29 (1991) 1279–1303.
[92] H.L. Gibbs, L. Sanz, J.E. Chiucchi, T.M. Farrell, J.J. Calvete, Proteomic analysis of ontogenetic and diet-related changes in venom composition of juvenile and adult dusky pigmy rattlesnakes (*Sistrurus miliarius barbouri*), J. Proteomics 74 (2011) 2169–2179.
[93] R.S. Thorpe, Geographic variation: a synthesis of cause, data, pattern and congruence in relation to subspecies, multivariate analysis and phylogenesis, Bolletino di Zoologia 54 (1987) 3–11.
[94] J. Diamond, Continental and insular speciation in Pacific land birds, Syst. Biol. 26 (1977) 263–268.